NATIONAL AERONAUTICS AND SPACE ADMINISTRATION

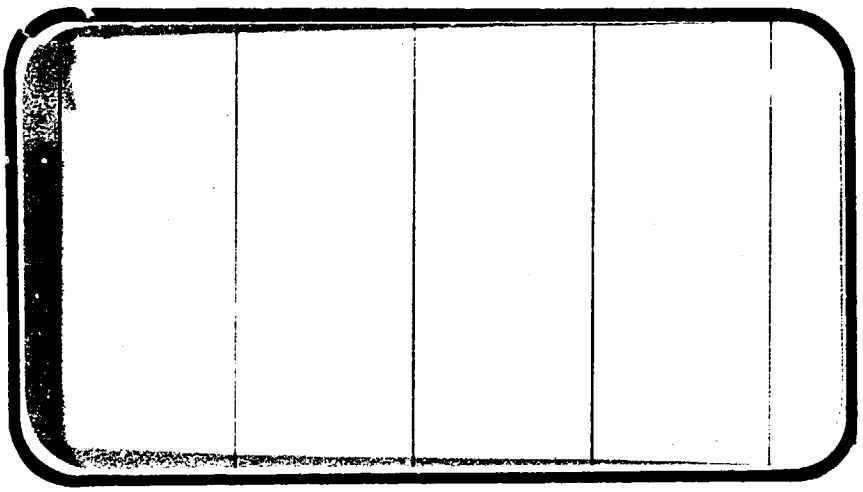

SPACE SHUTTLE

AEROTHERMODYNAMIC DATA REPORT

JOHNSON SPACE CENTER

HOUSTON, TEXAS

DATA MANagement services

SPACE DIVISION CHRYSLER CORPORATION

February, 1974

DMS-DR-2047
NASA CR-134,086

EFFECT OF WALL TO TOTAL TEMPERATURE RATIO VARIATION ON HEAT TRANSFER TO THE LEESIDE OF A SPACE SHUTTLE CONFIGURATION AT M = 10.3

By

James C. Dunavant
NASA Langley Research Center

Prepared under NASA Contract Number NAS9-13247

by

Data Management Services
Chrysler Corporation Space Division
New Orleans, La. 70189

for

Engineering Analysis Division

Johnson Space Center
National Aeronautics and Space Administration
Houston, Texas

WIND TUNNEL TEST SPECIFICS:

Test Number:	LARC/CFHT 98
NASA Series Number:	LA31
Date:	8/9/73 - 8/16/73 (48 Occupancy Hours)

FACILITY COORDINATOR:

David R. Stone
SSD, Hypersonic Analysis Section
Bldg. 1247-B, Room 120B
Mail Stop 163-A
Langley Research Center
Hampton, Va. 23665

Phone: (804) 827-2483

PROJECT ENGINEER:

James C. Dunavant
NASA Langley Research Center
SSD-Thermal Analysis Section
Mail Stop 408, Room 110A
Building 1251
Hampton, Virginia

Phone: (804) 827-3984

DATA MANAGEMENT SERVICES:

This document has been prepared by:

Maurice Moser, Jr.
Data Operations

This document has been reviewed and is approved for release.

for N. D. Kemp
Data Management Services

Chrysler Corporation Space Division assumes no responsibility for the data displayed herein other than its publication and distribution.

SUMMARY

An experimental study has been conducted of the influence of wall to total temperature ratio on the heat transfer to the leeside of an 040A space shuttle configuration. The heat transfer tests were made at a Mach number of 10 and a Reynolds number of 10^6 per foot for angles of attack from 0° to 30°. Range of wall to total temperature ratio was from 0.16 to 0.43. Where the heat transfer was relatively high and the laminar boundary layer attached, the local heat transfer decreased by about 20 percent as the wall to total temperature ratio was increased from the minimum to the maximum test value. In regions of separated flow and vortex reattachment, very low heating rates ($h/h_{r=1}$, ≈ .001) were measured at some conditions and indicate significant changes are occurring in the leeside flow field. No single trend of heat transfer variation with wall to total temperature ratio could be observed.

TABLE OF CONTENTS

LIST OF TABLES

LIST OF FIGURES

INTRODUCTION

With the introduction of reusable entry vehicles such as the space shuttles, weight and reusability of the thermal protection system become important factors. To design the leeside region without undue conservatism, an accurate prediction of the heat transfer which will exist in the flight entry environment must be made. It has become common practice to estimate the reentry flight heat transfer rates in many areas of the vehicle from hypersonic wind-tunnel tests made on small scale models under relatively cold flow conditions. The basis for this extrapolation is found in the similarity of the flight/wind-tunnel inviscid flow field and a viscous boundary layer similarity determined from theoretical calculations in simple inviscid flow situations. For laminar flow, the effects of boundary layer edge Mach number and wall-to-stream, total temperature ratio are small. For turbulent flow, the effects of the same two quantities are not negligible but can be accounted for in the extrapolation.

For the leeside of the shuttle, tests have shown a complex cross flow composed of separations and vortices. In this flow, boundary layer development can no longer be predicted from simple flow models, and the rationale for neglecting wall to total temperature ratio effects in laminar flow does not exist. In addition, at some leeside locations on the Apollo spacecraft, normalized heating rates during entry exhibited a decrease at the lower wall to total temperature ratios which was not present on the windward side of the spacecraft. Although the

change in the normalized heating rate cannot with certainty be attributed to a wall to total temperature ratio effect because Reynolds number and Mach number were also varying during the reentry, reasonable speculation exists that the normalized flight heating on the leeside at very low wall to total temperature ratios would be less than in the wind tunnel at high temperature ratios.

In the present experimental investigation, the influence of wall to total temperature ratio on leeside heat transfer is shown for an 040A configuration of the space shuttle. The range of temperature ratio of .16 to .43 was obtained by pre-cooling or pre-heating the model before test. The tests were conducted at a Mach number of 10.3 and a Reynolds number per foot of 1 million.

NOMENCLATURE

C_p	specific heat of model wall material
h	heat transfer coefficient
$h_{r=1'}$	stagnation heat transfer coefficient to scaled 1 ft. radius sphere
L	model length
R_e	Reynolds number
t	time
T	absolute temperature
X	axial length
α	angle of attack, deg.

λ model wall material thickness

ϕ peripheral angle measured from leeward meridian, deg.

ρ model wall material density

Subscripts:

aw adiabatic wall

w wall

MODEL DESCRIPTION

A .006 scale model of the 040A space shuttle configuration without the canopy as shown in figures 1(a) and 1(b) was used for the tests. The model was supported by two struts attached to the lower surface near the wing tips. All instrumentation was taken out through grooves in these struts. By mounting the model from the wing tips, the use of a center sting was avoided, thereby minimizing any possible sting effect on the wake and vortical flows on the leeside.

The model was cast in brass with a hollow core. In regions to be instrumented, wide slots were milled and covered with stainless steel sheets 0.022 inch thick in high heating regions and 0.010 inch thick in low regions. Chromel-alumel thermocouples were spot welded to the surface inside the model at locations shown in figure 2. Dimensions for the thermocouple locations are given in Table I.

TESTS

Facility

The tests were conducted in the Langley Research Center Continuous Flow Hypersonic Tunnel which has a calibrated Mach number of 10.33 at

the test Reynolds number of 1×10^6 per foot. The nominal total temperature for the tests was 1750° R. The tunnel is capable of operating in a continuous mode or a blowdown mode; these tests were made in the continuous operating mode. A more detailed description of the tunnel is given in reference 1.

Methods

The transient calorimeter technique was used to measure the heat transfer to the model. The model is located initially in an injection chamber adjoining the test section at a pressure equal to the test section static pressure. With hypersonic flow established in the test section, the model is rapidly injected to the center of the test section, and the temperature data were recorded at a rate of 20 samples per second.

The tests were conducted over a range of wall temperatures from approximately 280° R to 750° R (T_w/T_t = .16 to .43) by cooling or heating the model prior to injection. The present injection mechanism contains a door which can seal the injection chamber from the test section pressure, and the entire injection chamber could be rotated to expose the model to nominal room conditions. To obtain tests at model wall temperatures above room temperature, the model was heated with small hot-air blowers with the injection chamber rotated toward the room. Because the model slowly lost heat between the heat cycle and test, the desired test temperatures were exceeded in the heating cycle. After model preheat, the injection chamber was rotated to the test section position, bled down to test section pressure, and the model injected for test.

To obtain low temperature, the model was cooled with a mixture of gaseous and liquid nitrogen which was introduced to the hollow core

of the model through a small tube inserted in the base.

To prevent frost formation on the model, cooling was accomplished with the injection chamber turned toward the test section and bled down to approximately test section static pressure. A door between the test section and the injection chamber always remained closed until just prior to injection. Because these measures did not fully prevent frost formation, an aluminum foil glove was fitted over the model, which remained in place during the cooling cycle. Upon injection, the glove was stripped off and the model entered the test section in a clean, frost-free condition.

Several minutes were allowed after both the heating and cooling cycles for the model to come to near isothermal condition before injecting into the stream for the heat transfer test. Particular care was taken to insure that no liquid nitrogen remained inside the model; this could always be detected by monitoring the model temperature distribution. If liquid nitrogen was present after the cooling cycle, the temperature remained constant at 141° R.

Data Reduction

A quadratic least squares curve was fitted to a 1-second (20 data points) interval of data. The first 1/2-second of data immediately following model injection was ignored to allow heating conditions to stabilize. The rate of change of temperature with time ($\partial T_w/\partial t$) was evaluated analytically from the curve fit expression at the initial point and heat transfer coefficient was calculated from the expression:

$$h = \frac{\rho C_p \lambda \frac{\partial T_w}{\partial t}}{T_{aw} - T_w}$$

Adiabatic wall temperature (T_{aw}) was based on free stream conditions and an assumed recovery factor of .85.

All the heat transfer data are non-dimensionalized by the stagnation heat transfer coefficient to a scaled 1-foot radius sphere. Thus, the radius of the reference sphere in these tests is .006 foot. The reference heat transfer coefficient was calculated from the Fay and Riddell expression for a wall temperature of 530° R for all tests.

Data Accuracy

Because of the need to establish high and low model temperature conditions before injection, these tests were subject to greater inaccuracy than those following normal test procedures. After termination of the pre-cooling/heating cycle and several minutes for model thermal conditions to stabilize, it was found that the cold model gained heat and the hot model lost heat. This heat loss or gain resulted from convective exchange with the air in the injection box, radiation from/to the box and conduction through the model skin and support struts. Immediately before injection, the pressure in the injection box was approximately the tunnel static pressure (.02 psia) and air temperature probably near room temperature. Thus, natural convection was thought to be small as was radiation since both model and surrounding box temperatures were low. Conductive heat exchange to instrumented skin is, of course, a result of temperature gradients in the model. The center-line leeside temperature distributions which existed at model injection are

shown for the $\alpha = 0°$ tests in figure 3. The support strut, which was not directly cooled in the low temperature tests, provided the source of heat which caused aft temperatures to be high relative to forward location. Heat was applied directly to both the model and strut for the high temperature tests and a more uniform model temperature was obtained.

A measure of the total heat exchange to the model at 1 second before injection is shown in figure 4. Heating rate has been obtained using the same data system and procedures as would be used in a normal test with the exception that the model is inside the injection box and experiences none of the M = 10 airstream heat loads. Heating rates have been normalized to the same free stream reference sphere heating rates described in Data Reduction and are hence directly comparable to the other heat transfer data. The heating rates are positive at low wall temperatures where the model is gaining heat and negative at high temperatures for heat loss. At ambient temperatures ($T_w/T_t \approx .32$), the results indicate the model was also gaining heat. At all wall temperatures, there is a large amount of scatter in the leeward meridian data shown in figure 4; however, the majority of the data are contained between $h/h_{r=1'} = \pm.002$. The significance of these residual heating/cooling rates must be measured in relationship to aerodynamic heating rates measured after injection and shown in later sections of this report. Furthermore, this heating/cooling may change significantly in the two seconds time difference between this preliminary measurement and the stream heat transfer measurement. In general, these residual heating/

cooling rates can be a sizeable fraction of measured heating rates on the leeside in low heating areas. But in higher heating areas, they are of little importance to the accuracy of the results.

No correction to the measured heating rates have been made for conduction or radiation.

RESULTS AND DISCUSSION

For the various wall to total temperature ratios tested, heat transfer distributions along the leeward meridian are shown for the four angles of attack (α = 0°, 10°, 20°, and 30°) in figures 5 through 8. The heating for the three farthest aft thermocouples (X/L > .8) was measured 36° off the leeward meridian because of interference with the vertical tail. Each heating distribution is identified by a single wall-to-total temperature ratio which is the average of four representative centerline leesurface measurements.

Past experience indicates that the flow over the model for the test conditions (M = 10.3 and unit Reynolds number of 10^6 per foot) would be laminar on both the windward and leeward surfaces.

The α = 0 heating distributions, figure 5, are believed to be the result of fully attached laminar flow; no significant effect of wall to total temperature ratio can be seen either in the heating level or the distribution of heating. Increasing the angle of attack to 10° reduces the heating on the conical region forward of the shoulder (X/L ≈ .4) by a factor of about two, figure 6; the heating is affected by temperature ratio only in the region after the expansion over the shoulder where the

heating drops nearly to zero ($h/h_{r=1}$, < .001) for wall temperature ratios equal to or greater than .319. Further increases in angle of attack often result in increased leeward heating and several of these are believed to be the result of vortex formation. One such vortex occurs in the region between X/L = .1 and .25 at 30° angle of attack. At this angle of attack, the leeward centerline of the nose section is inclined about 10° away from the flow. The increase in heating over the α = 20° heating and the shape of the chordwise heating distribution is similar to that obtained in tests of this configuration at M = 6 (Ref. 2) where the vortex formation was identified in oil flow tests. Over the forward section, the heating levels and shape of the heating distributions are nearly the same at all wall to total temperature ratios at any single angle of attack.

Aft of the shoulder expansion (X/L ≈ .4), several notable increases in heating occur. In the two coldest wall temperature α = 30° tests (T_w/T_t = .171 and .206, figures 8(a) and 8(b)), the heat transfer between X/L = .45 and .7 exceeds that at α = 0°. The fact that this increase occurs after the low heat transfer over the expansion on the shoulder strongly suggests that it is the result of separation and vortex formation. This same pattern occurs at several wall temperature ratios at α = 20° (see figures 7(c) and 7(d)). Because this vortex occurs sporadically, it is believed that it likely results from some factor other than wall-to-total temperature ratio.

In figures 9 through 12, the heat transfer ratio, $h/h_{r=1'}$, is plotted as a function of wall to total temperature for the thermocouples located off the lee meridian and the lee meridian ones located at approximately the same chordwise station.

Nearly all of the results in the higher heating regions ($h/h_{r=1'} > .01$) show a small effect of wall to total temperature ratio. The local heat transfer coefficient decreases by about 20 percent between the minimum and maximum temperature ratios of these tests. This trend of lower heating at higher wall temperatures is similar to that which has been well established for laminar flat plate flow. The lower heating rates at the higher angles of attack show the sporadic heating variation noted earlier to be associated with separation.

Further evidence of the vortex formation aft of the shoulder at $\alpha = 30°$ is seen in the variation in heating with the peripheral angle ϕ in figure 12(c) and 12(d). Heating on the lee meridian ($\phi = 0°$) is frequently greater than a short distance off the meridian ($\phi \approx 30°$). Where vortices are present, separation will occur off the meridian, resulting in heating lower than at the reattachment point on the meridian.

In the separated flow and vortex attachment regions on the leeside, no single trend of heat transfer rate with wall to total temperature ratio is present in these tests. The presence or absence of vortices in the leeside flow does not appear to be strongly dependent on wall temperature. Changes in wall temperature often appear to alter the leeside flow, but whether a wall temperature decrease causes a vortex to intensify or disappear seems to be more dependent on geometric factors such as location and angle of attack than solely related to wall to total temperature ratio.

SUMMARY OF RESULTS

An experimental study has been conducted of the influence of wall to total temperature ratio on the heat transfer to the leeside of an 040A space shuttle configuration. The heat transfer tests were made at a Mach number of 10 and a Reynolds number of 10^6 per foot for angles of attack from 0° to 30°. The model was precooled or preheated before the testing to produce results over a range of wall to total temperature ratios from 0.16 to 0.43. From past experience, it is expected that the boundary layer over the model would be laminar for the test Reynolds number and Mach number. The heat transfer results of these tests show that:

1. On the leeside at 0° angle of attack, and at higher angles of attack on the sides where the heat transfer is relatively high ($h/h_{r=1}, \geq .008$) and the flow is believed to be attached, the local heat transfer coefficient decreased by about 20 percent as the wall to total temperature ratio was increased from the minimum to maximum test values.

2. At 30° angle of attack, the heating over the forward nose section increased to a value greater than at 20° as a result of a vortex in this region. Evidence of vortices aft of the shoulder expansion is also present at the high angle of attack.

3. In regions of separated flow and vortex reattachment, very low heating rates ($h/h_{r=1}, \approx .001$) were measured at some conditions and indicate significant changes are ocurring in the leeside flow field. No single trend of heat transfer variation with wall to total temperature ratio could be observed.

REFERENCES

1. Dunavant, James C.; and Stone, Howard W.: Effects of Roughness on Heat Transfer to Hemisphere Cylinders at Mach Numbers 10.4 and 11.4. NASA TN D-3871, March 1967.

2. Miyazawa, Masafumi: Lee-Surface Flow Phenomena Over Space-Shuttle-Oriented Configurations at Large Angles of Attack and Hypersonic Speeds. Proposed Doctoral Thesis, New York University.

TABLE I - THERMOCOUPLE LOCATIONS

T. C. NUMBER	X/L	Φ
1	.028	0°
2	.060	
3	.092	
4	.124	
5	.155	
6	.187	
7	.219	
8	.250	
9	.282	
10	.336	
11	.383	
12	.447	
13	.510	
14	.514	
15	.637	
16	.684	
17	.732	
18	.804	36°
19	.874	
20	.946	
21	.168	39°
22	↓	84°
23	↓	128°
24	.326	42°
25	↓	77°
26	↓	107°
27	.489	29°
28	↓	68°
29	↓	94°
30	.694	34°
31	↓	72°
32	↓	102°

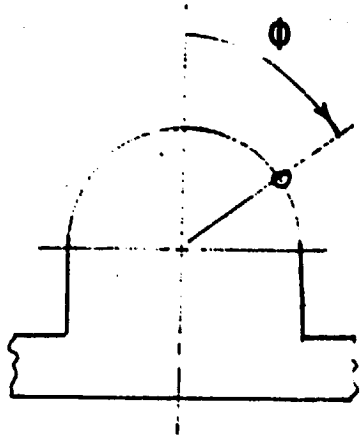

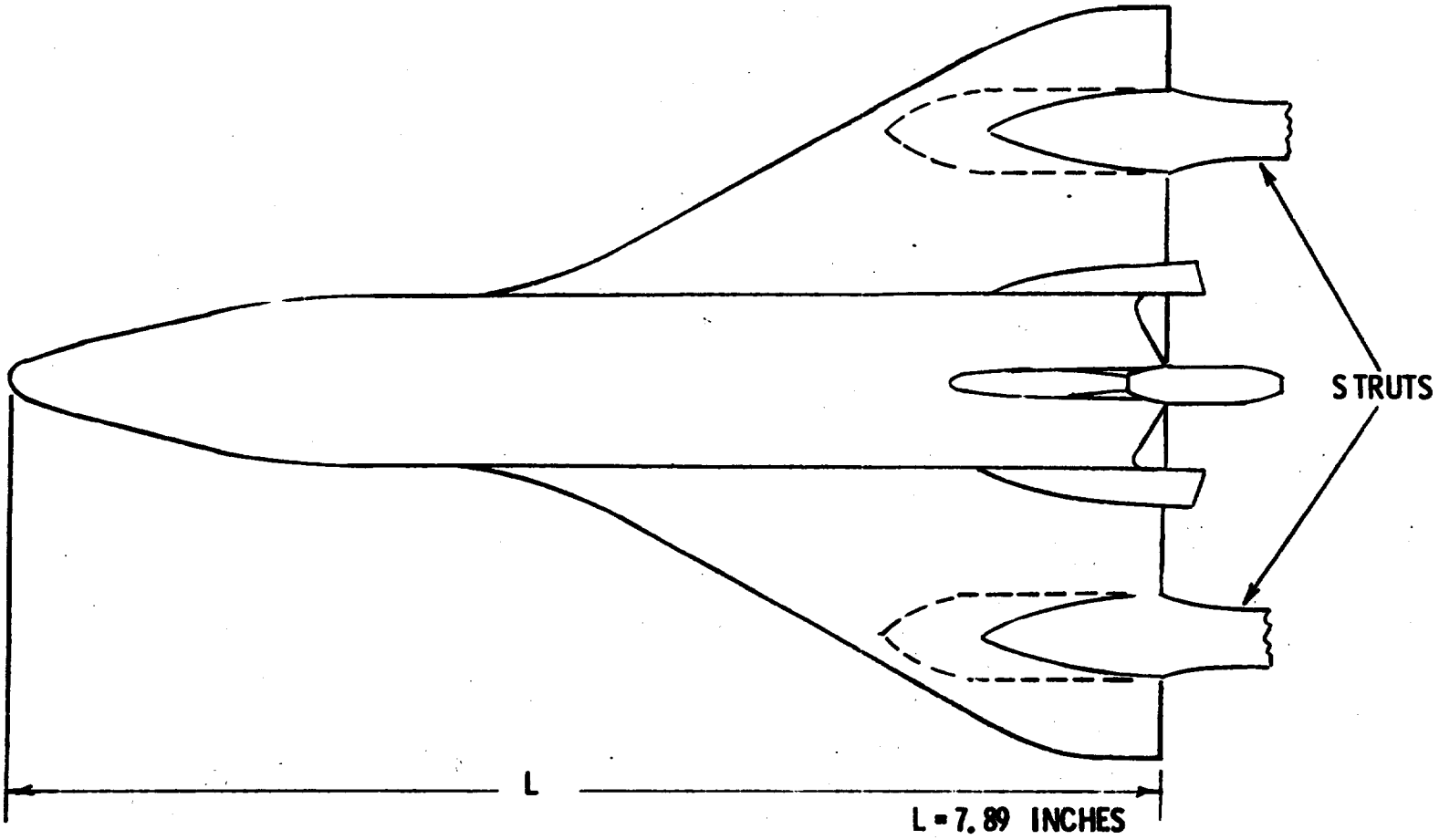

(a) Planform view

Figure 1. - Model configuration.

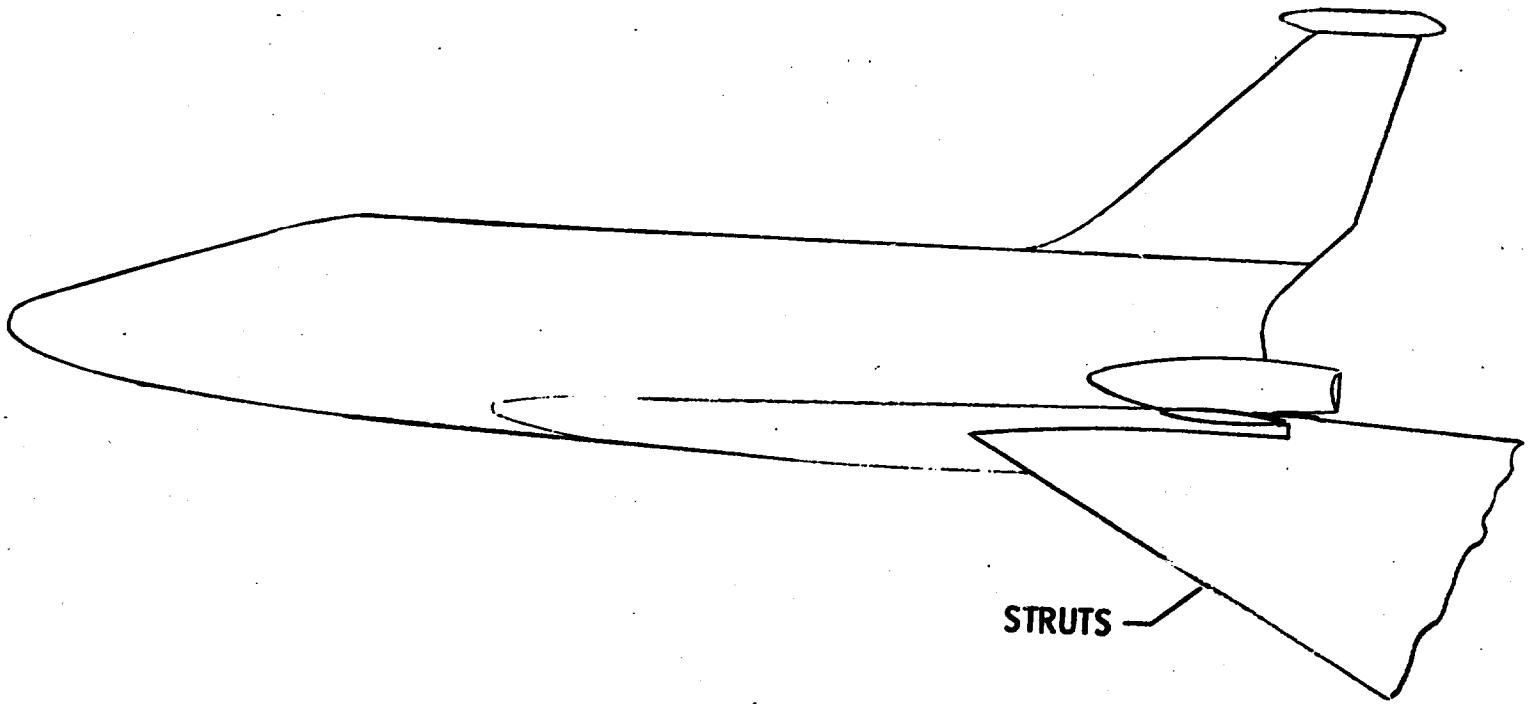

(b) Side view

Figure 1. - Concluded.

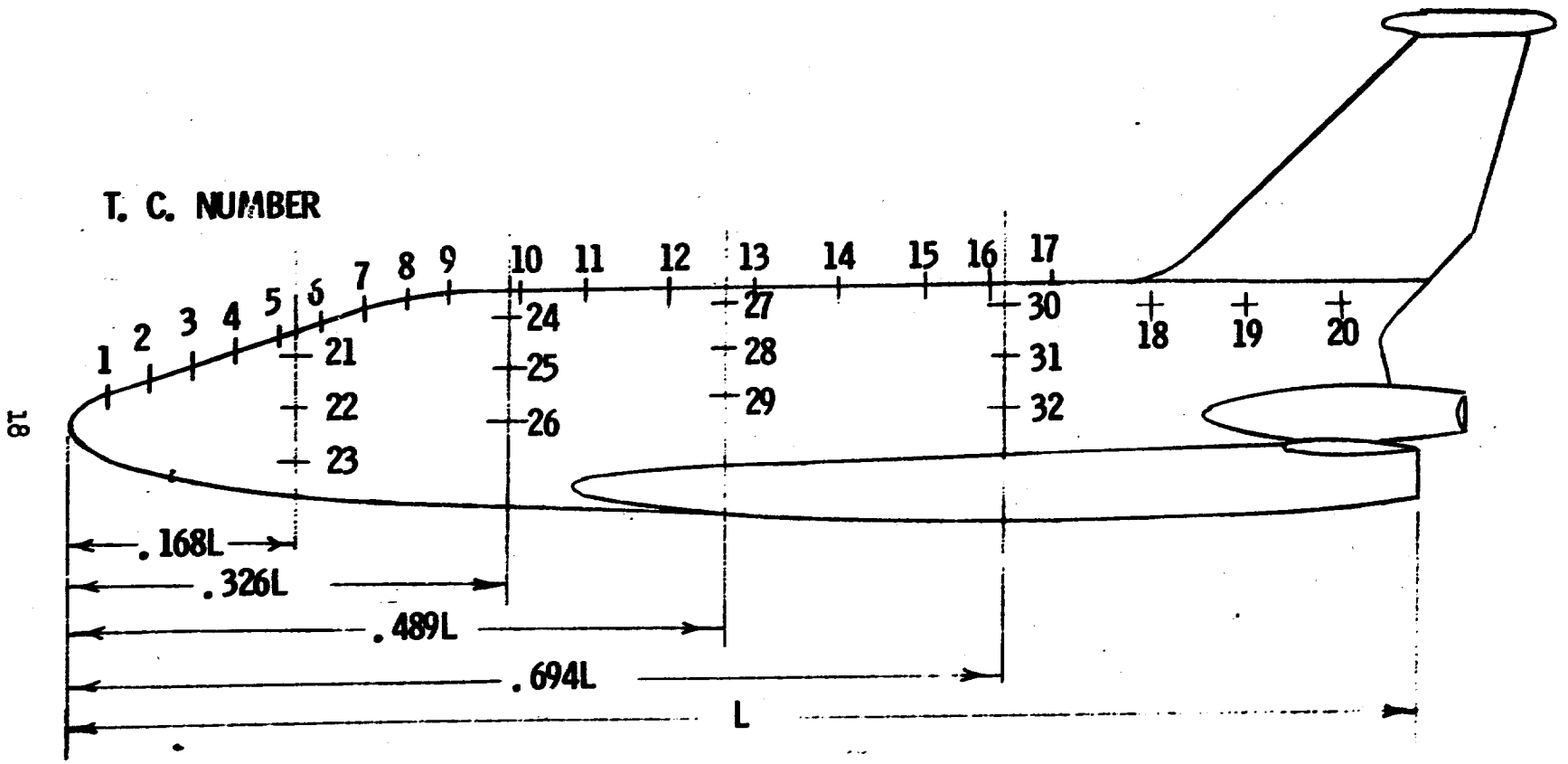

Figure 2. - Thermocouple locations.

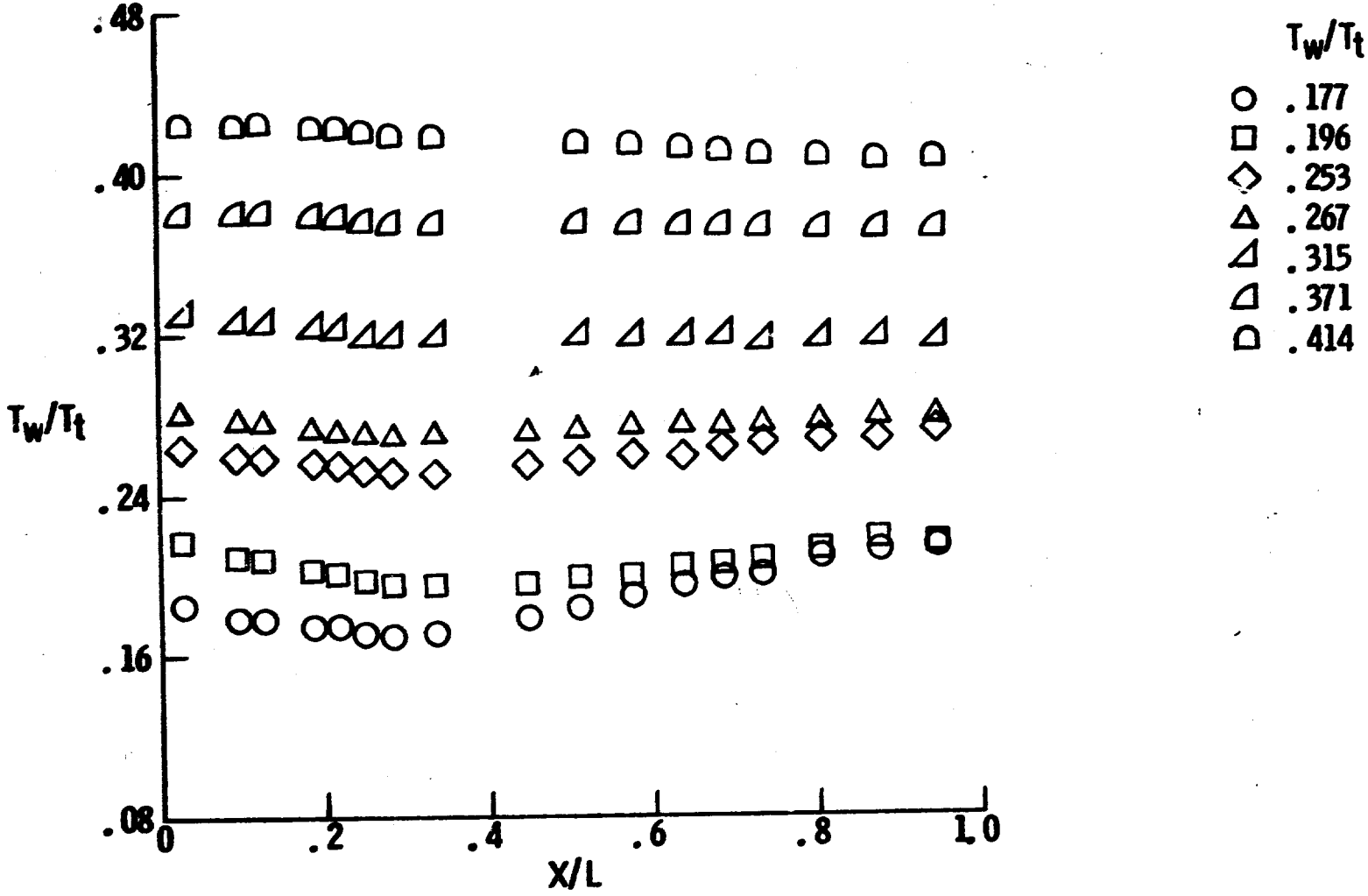

Figure 3. - Leeside centerline wall temperature distributions, $\alpha = 0°$.

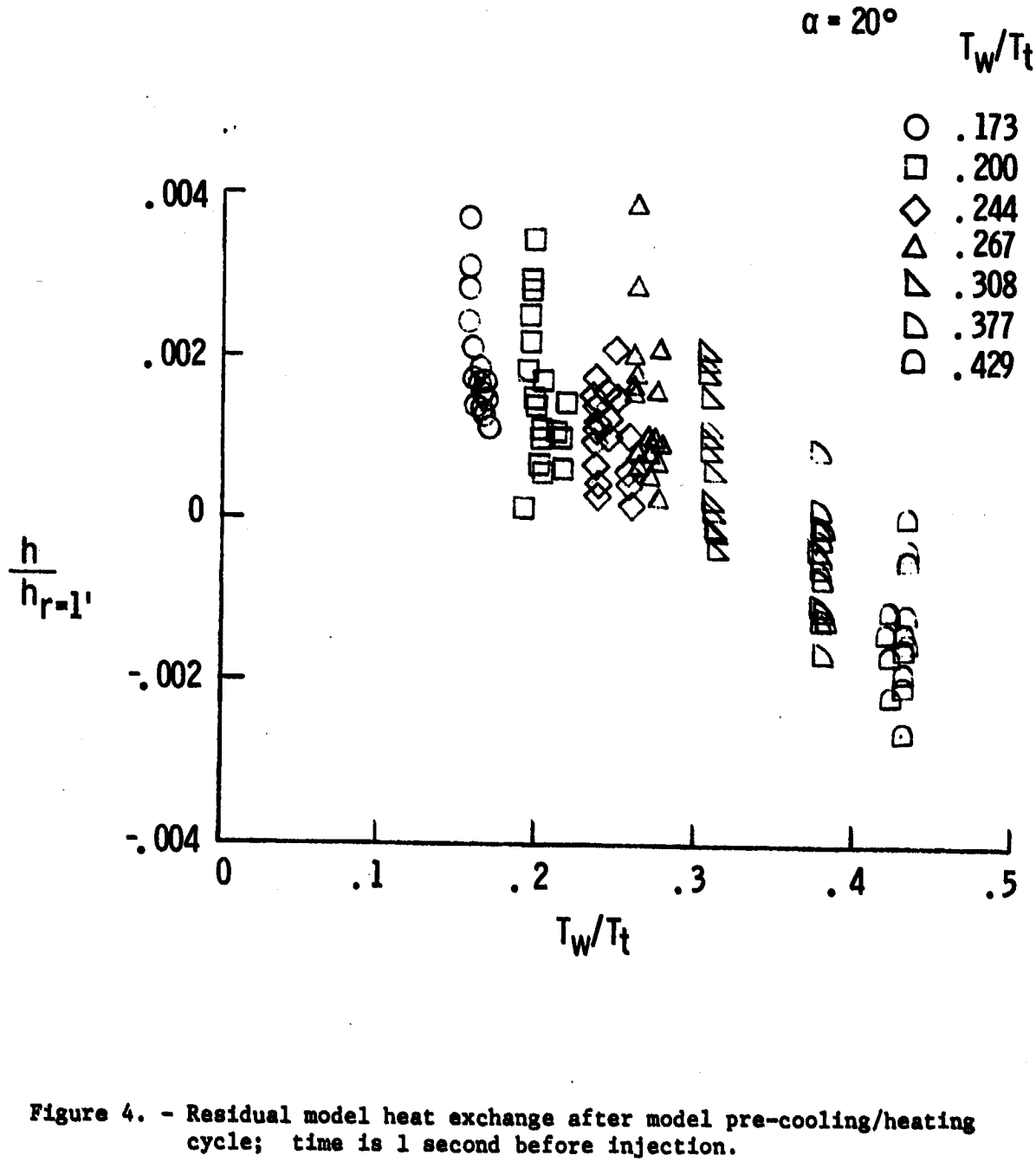

Figure 4. - Residual model heat exchange after model pre-cooling/heating cycle; time is 1 second before injection.

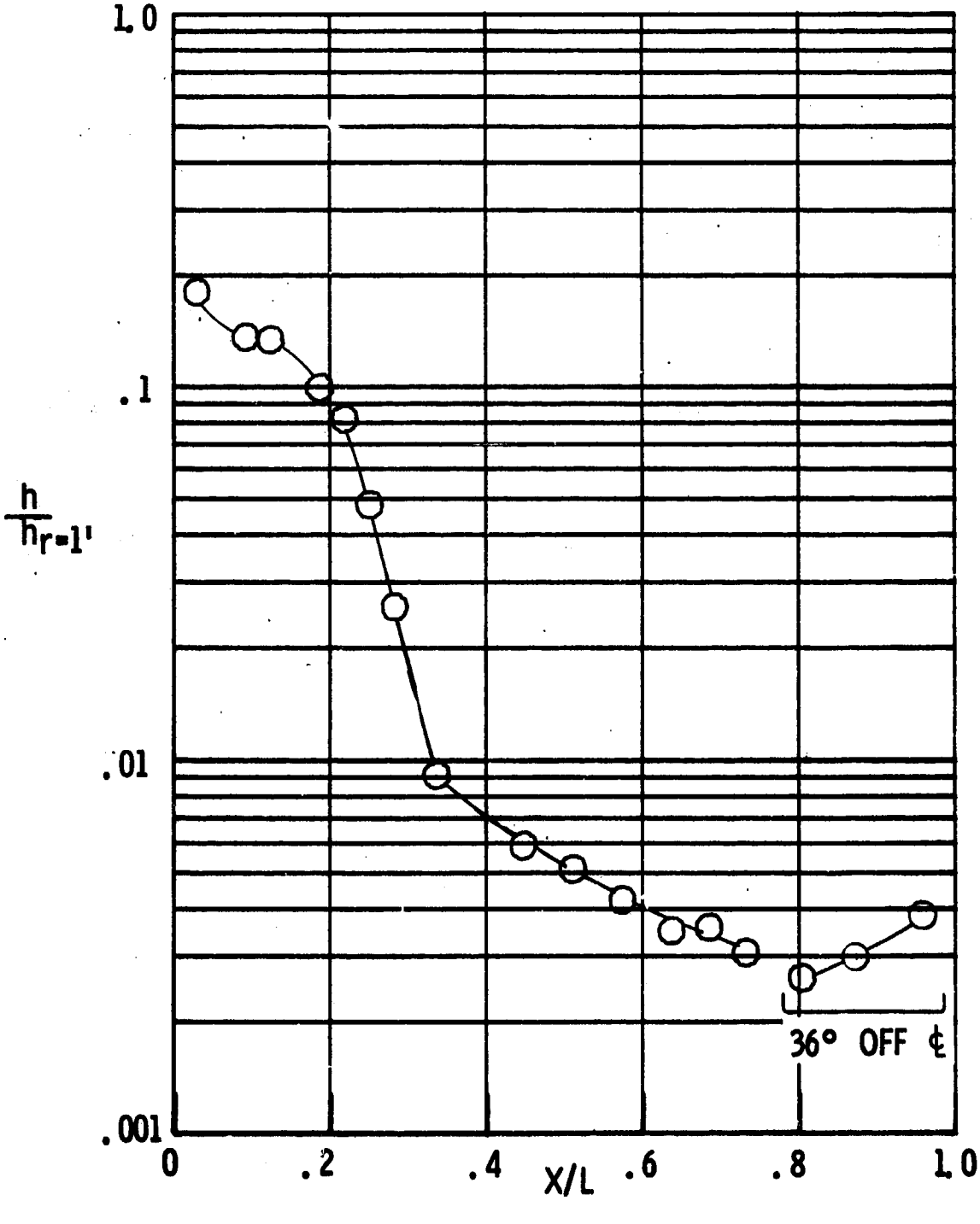

(a) $T_w/T_t = 0.177$

Figure 5. - Leeside centerline heat transfer distributions, $\alpha = 0°$.

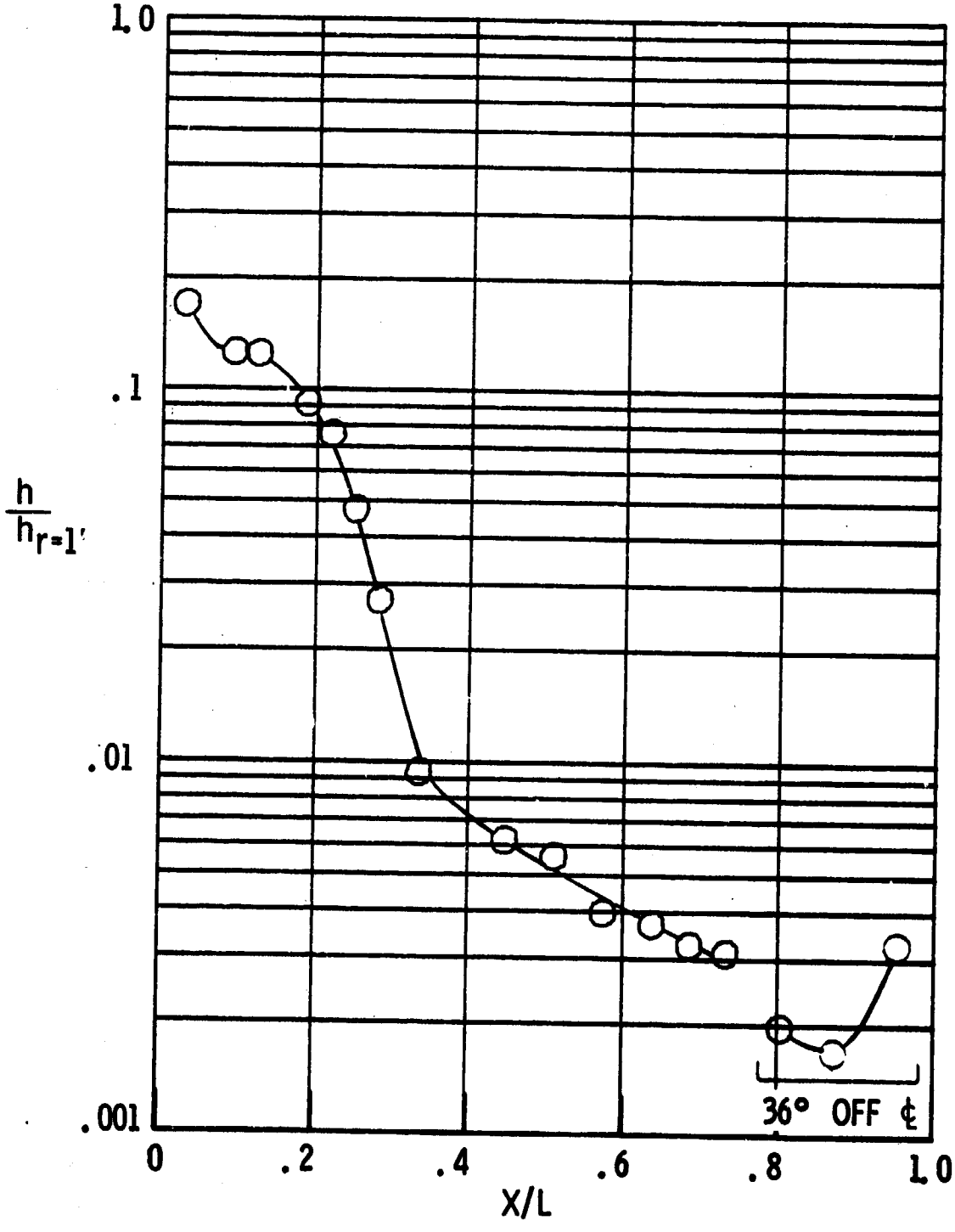

(b) $T_w/T_t = 0.196$

Figure 5. - Continued.

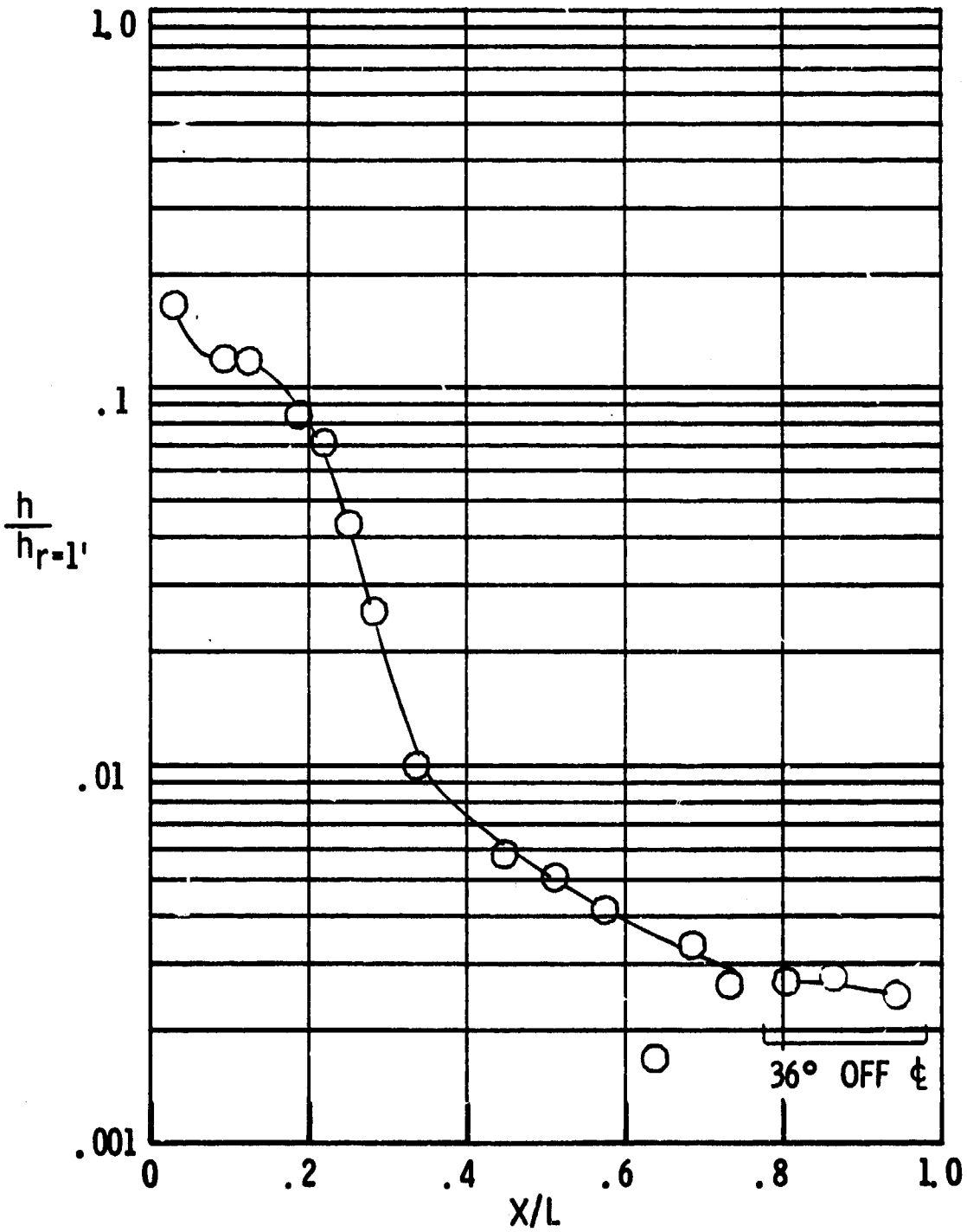

(c) $T_w/T_t = 0.253$

Figure 5. - Continued.

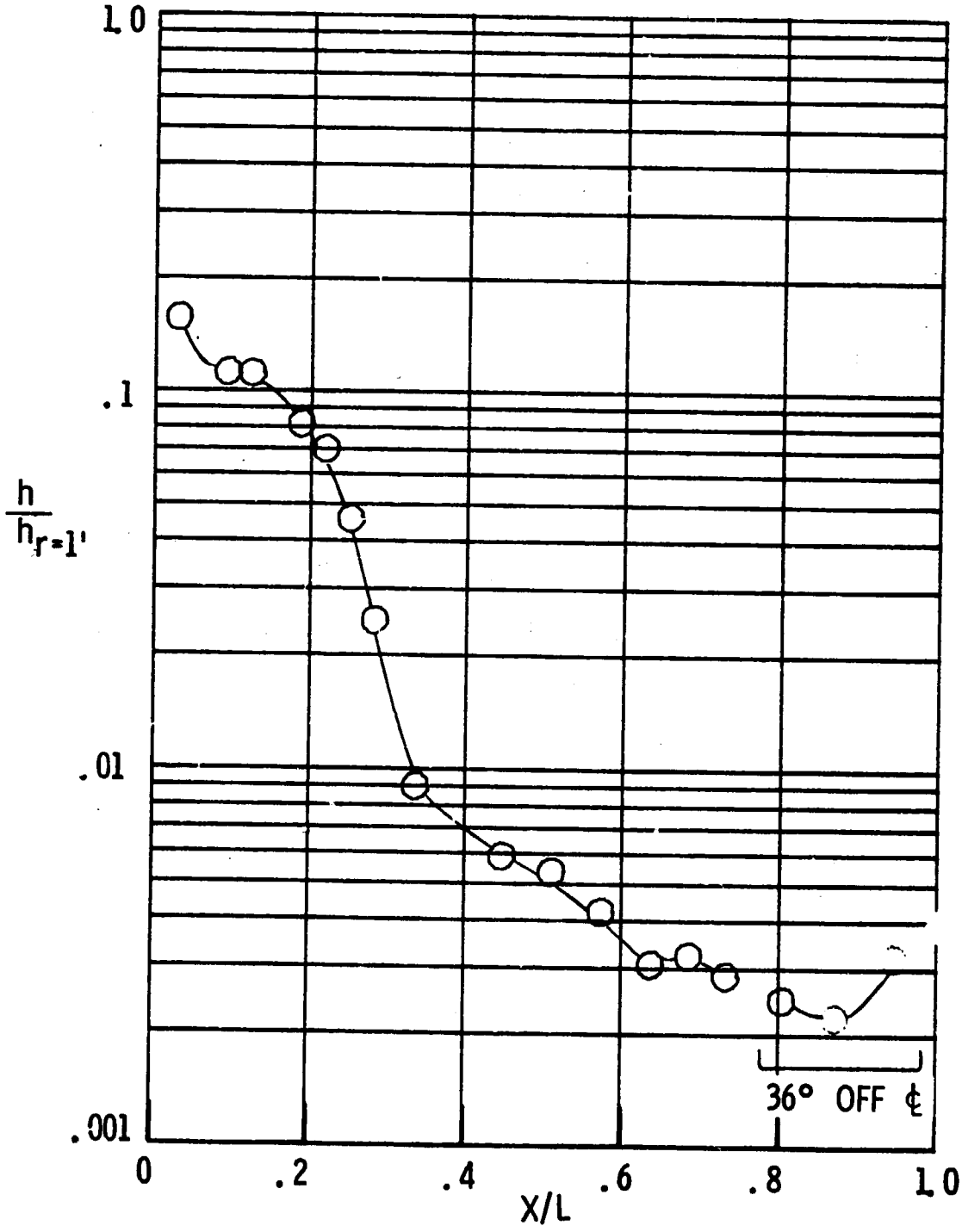

(d) $T_w/T_t = 0.267$

Figure 5. - Continued.

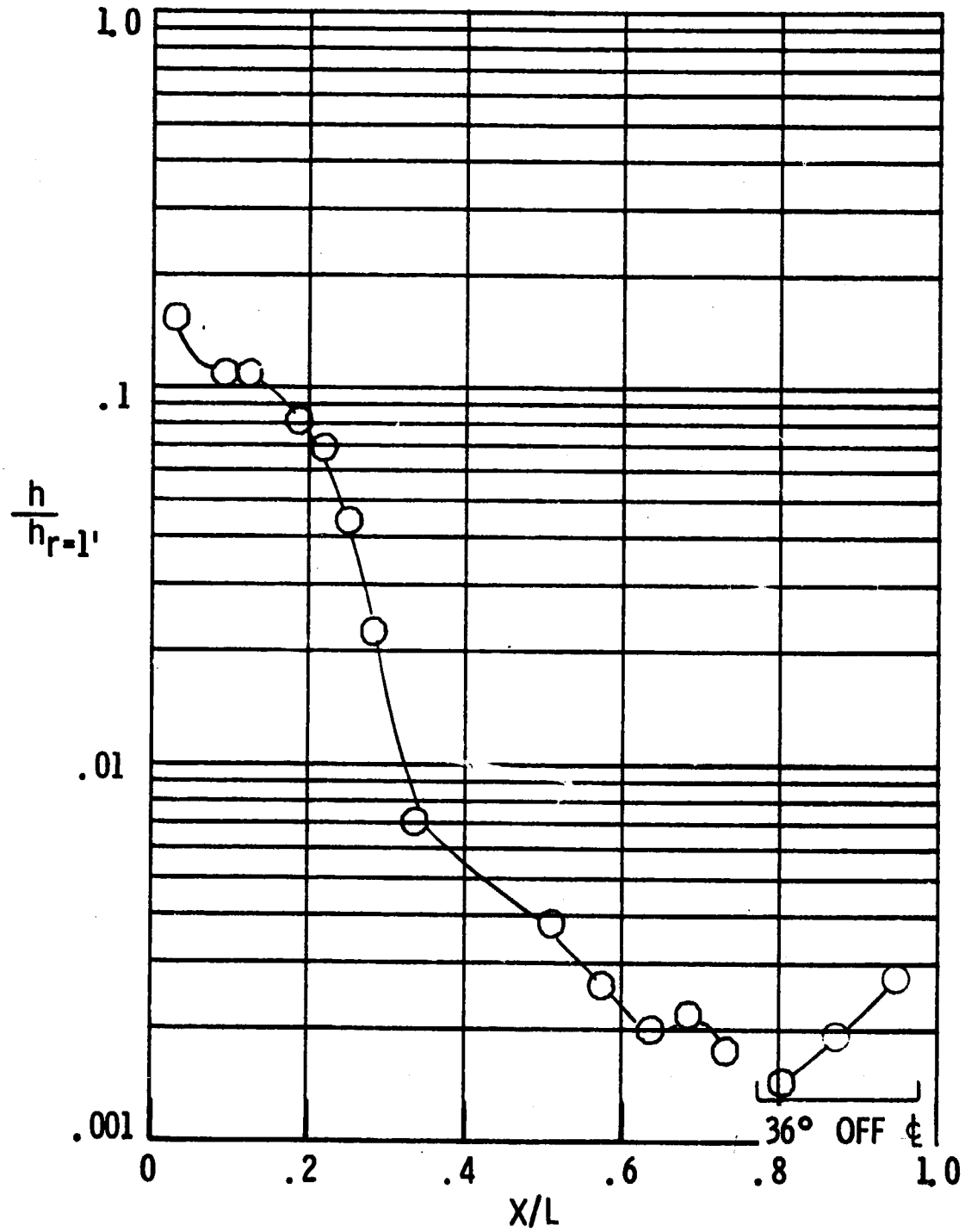

(e) $T_w/T_t = 0.315$

Figure 5. - Continued.

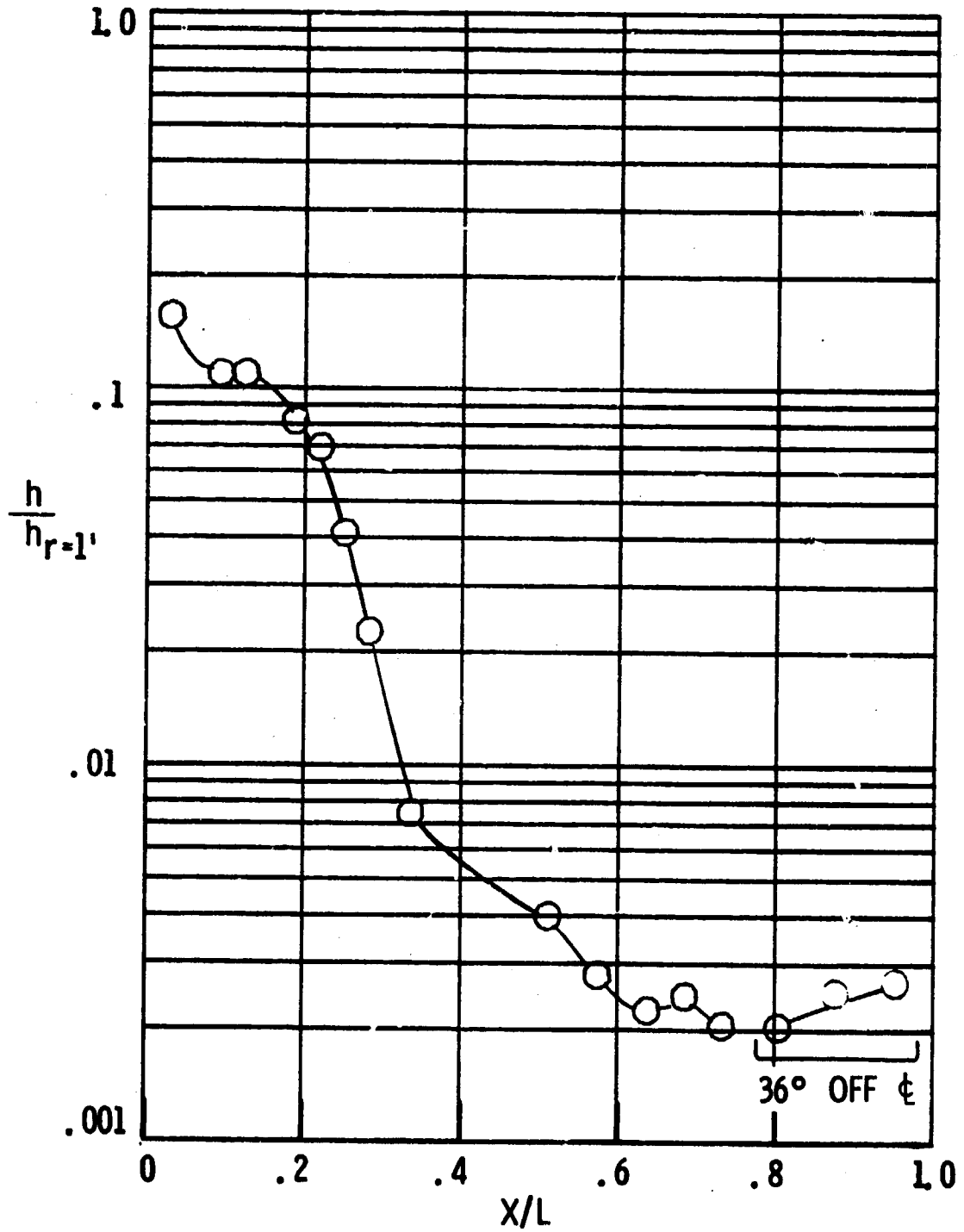

(f) $T_w/T_t = 0.371$

Figure 5. - Continued.

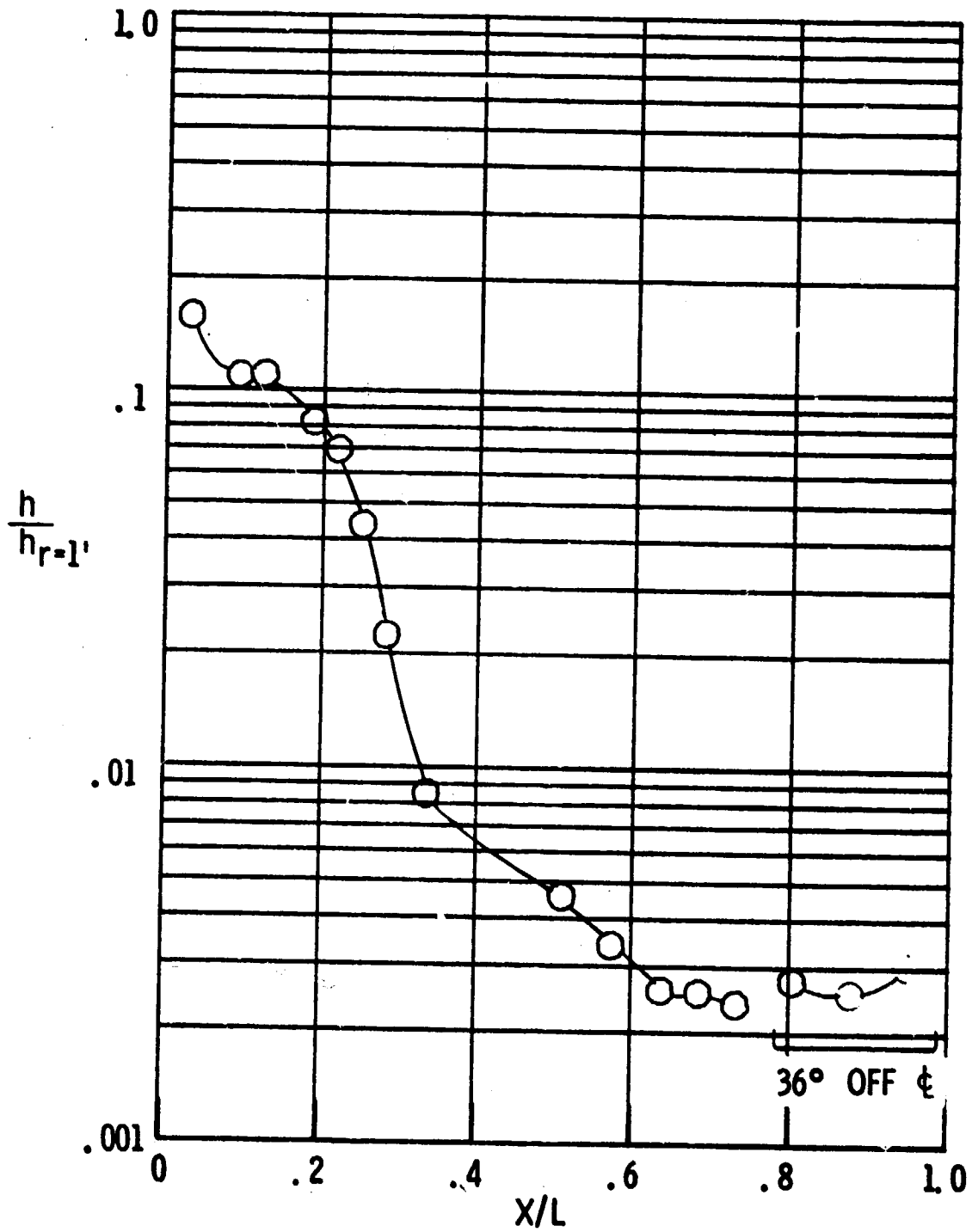

(g) $T_w/T_t = 0.414$

Figure 5. - Concluded.

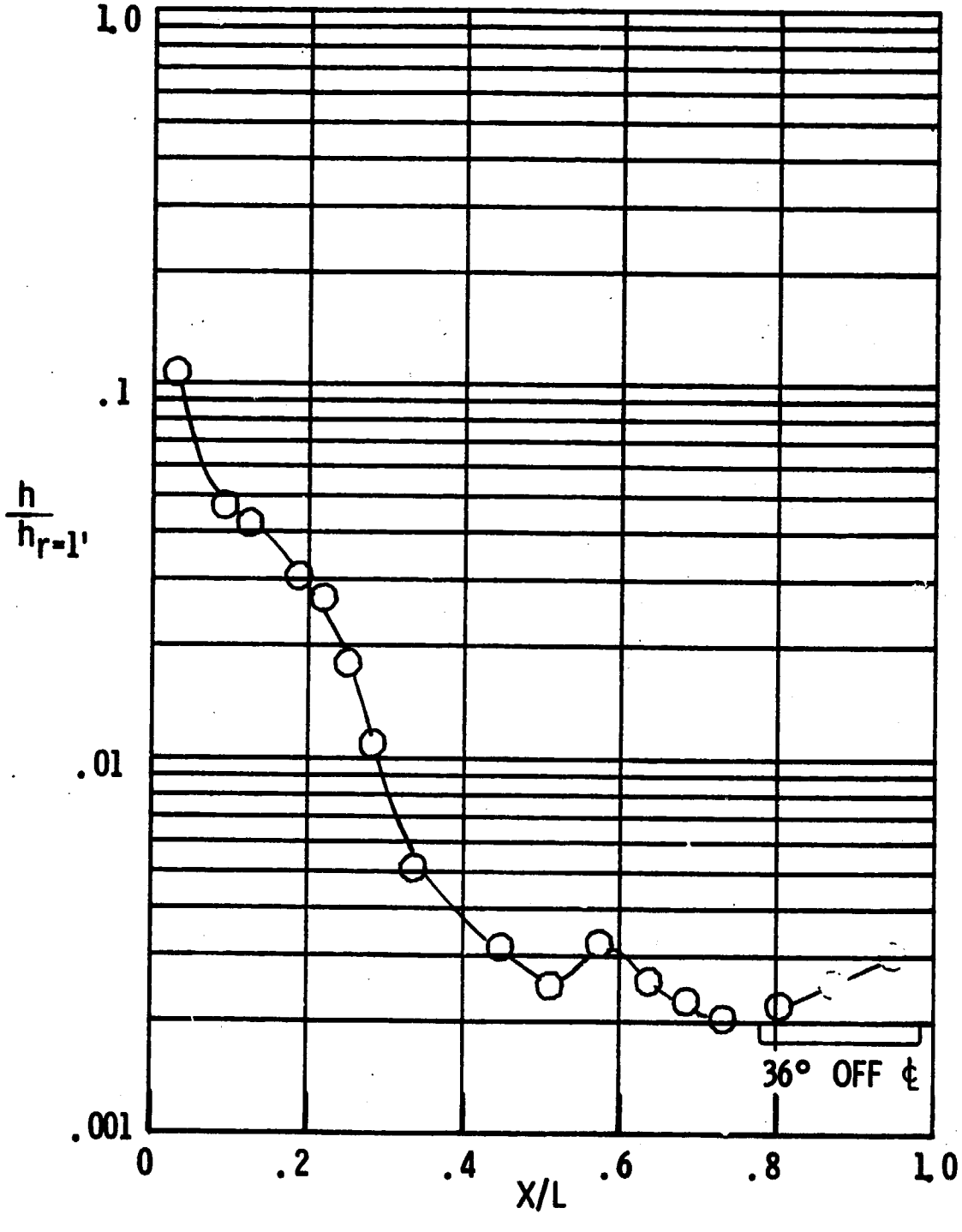

(a) $T_w/T_t = 0.156$

Figure 6. - Leeside centerline heat transfer distribution, $\alpha = 10°$.

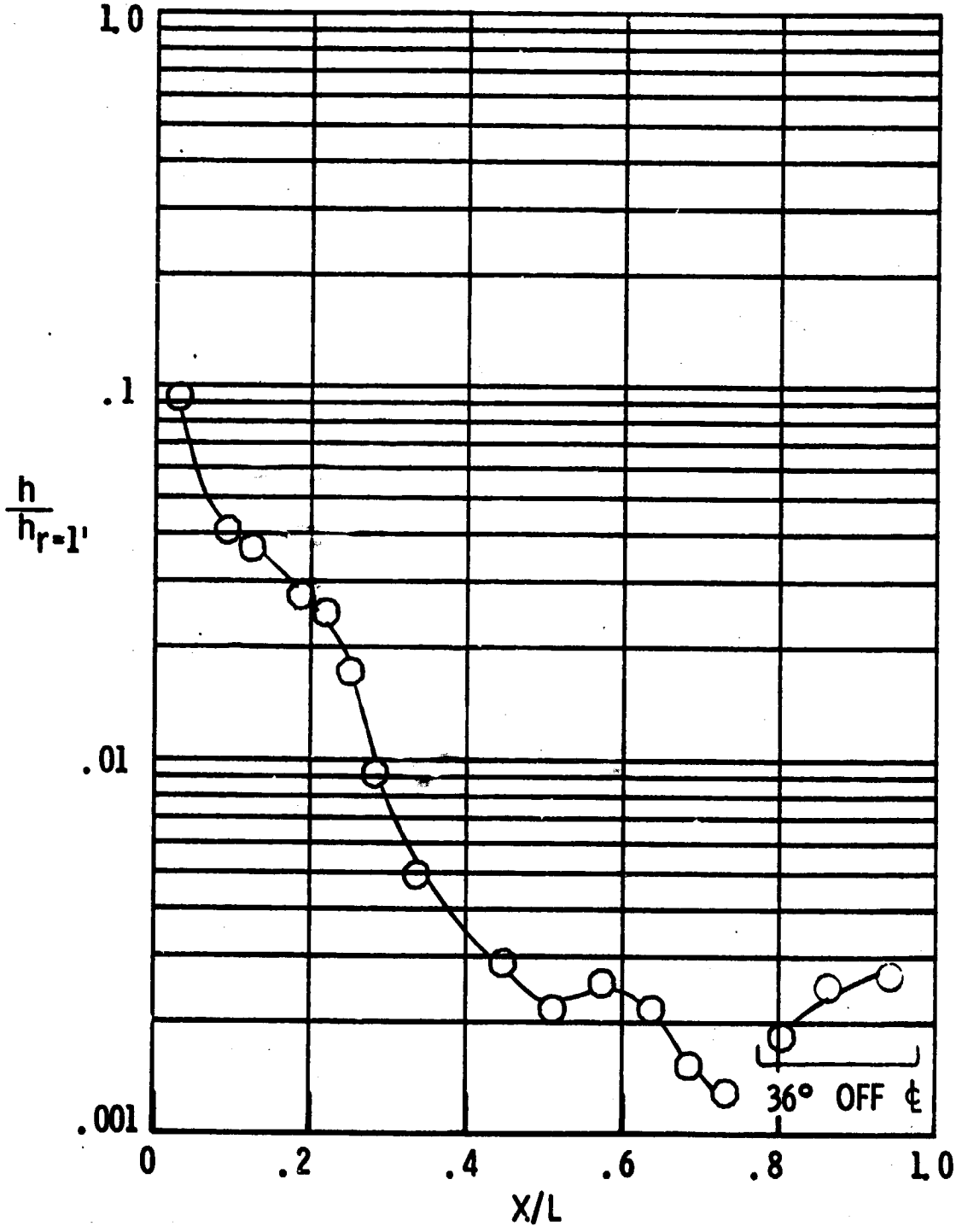

(b) T_w/T_t = 0.227

Figure 6. - Continued.

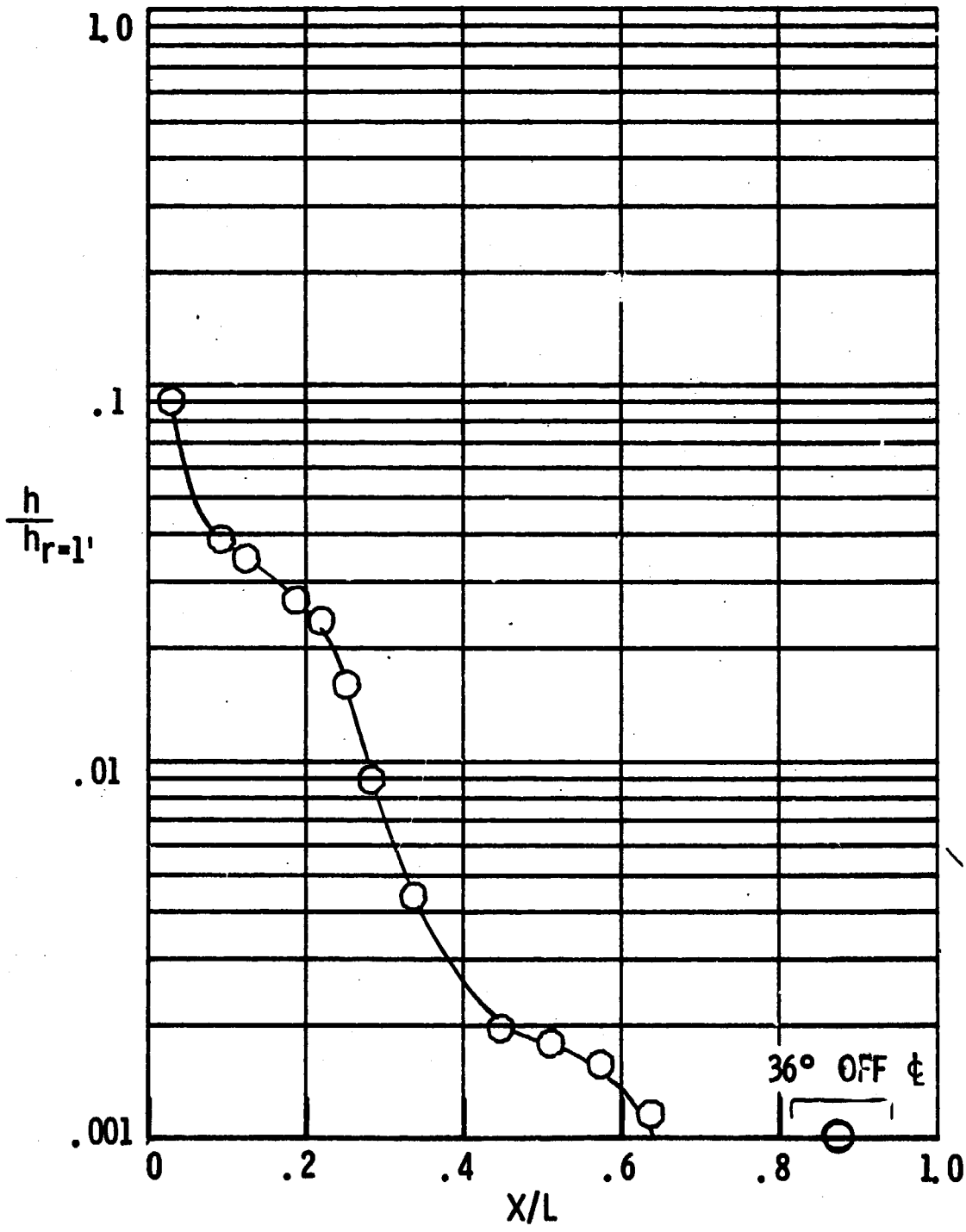

(c) $T_w/T_t = 0.233$

Figure 6. - Continued.

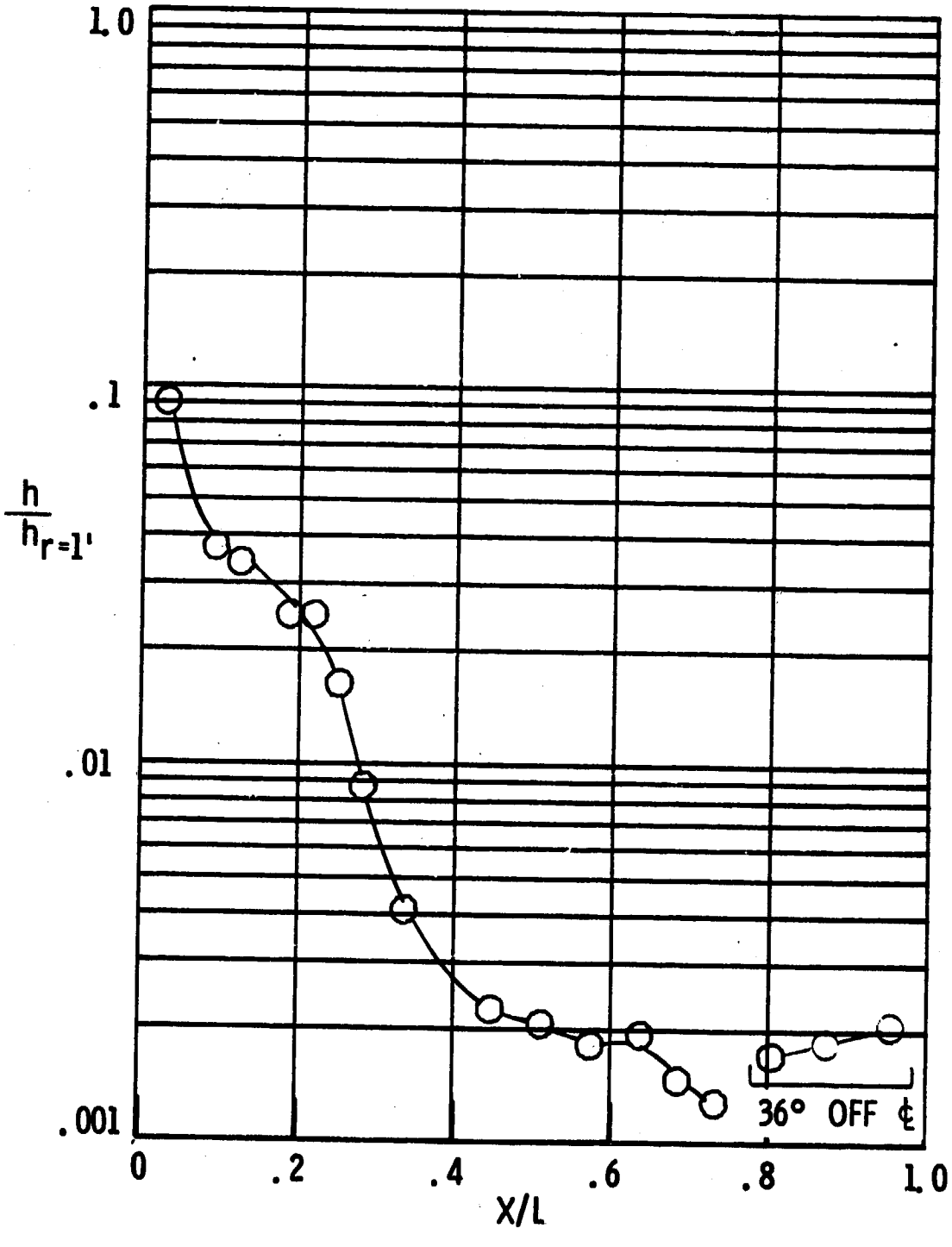

(d) T_w/T_t = 0.270

Figure 6. - Continued.

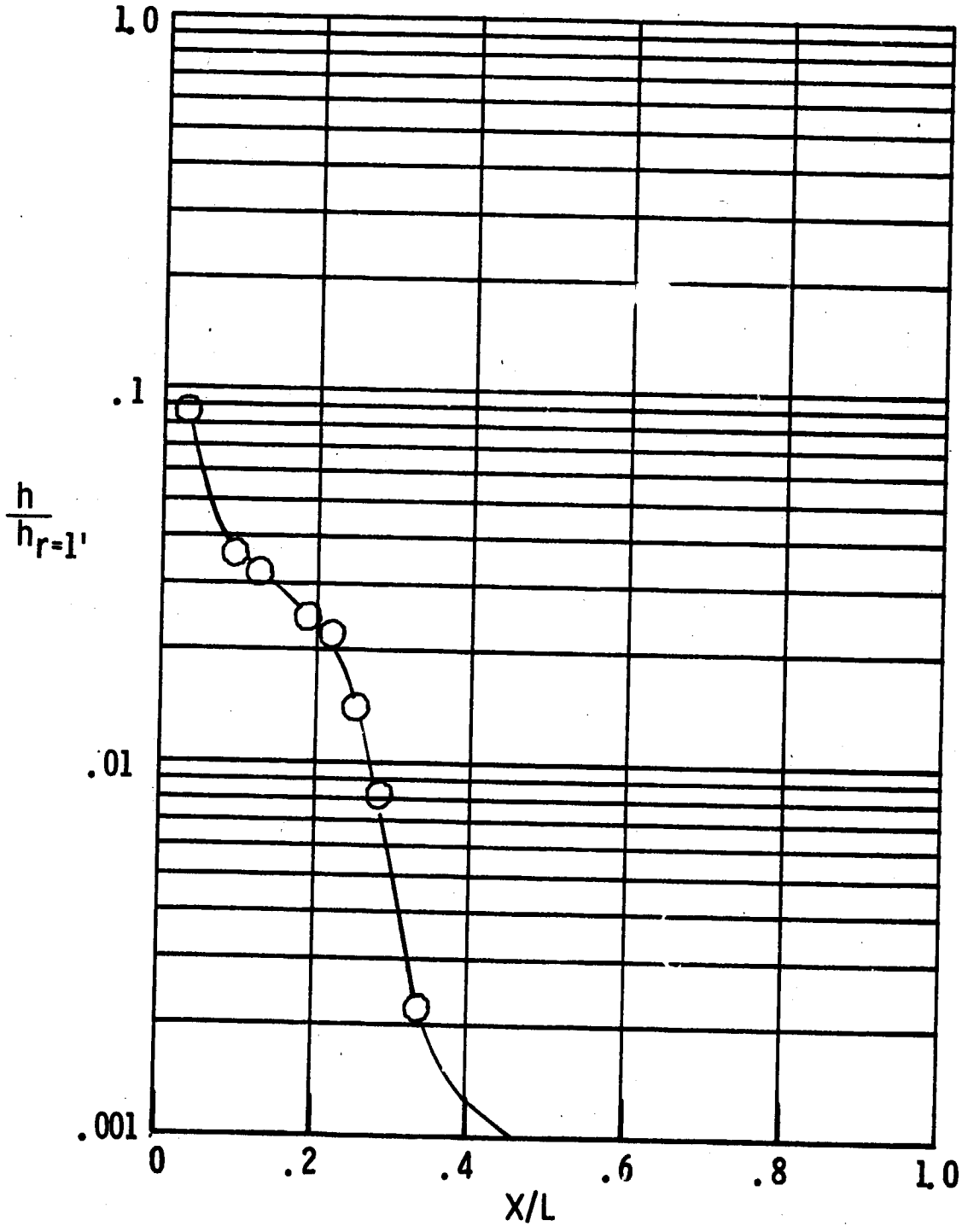

(e) $T_w/T_t = 0.319$

Figure 6. - Continued.

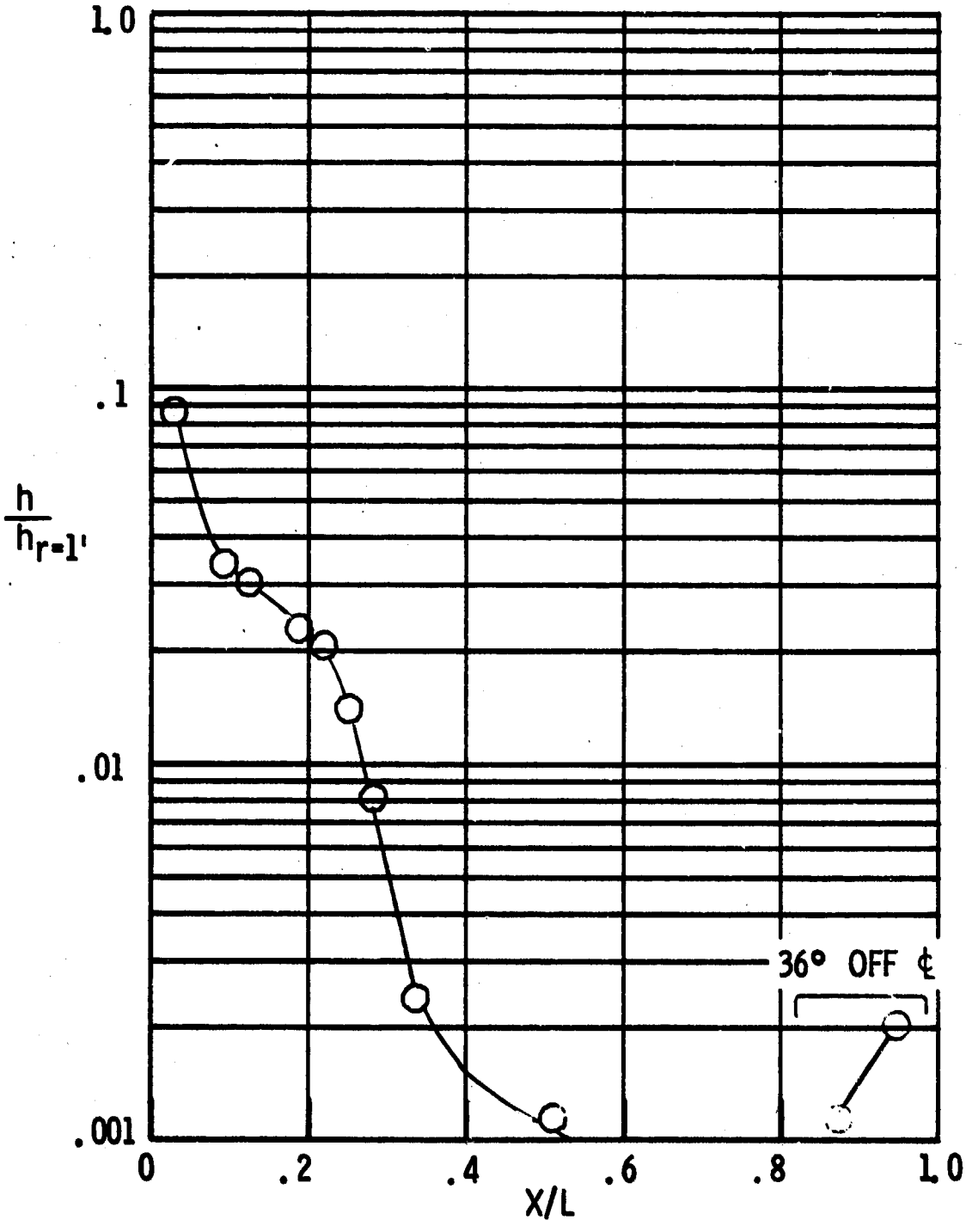

(f) $T_w/T_t = 0.369$

Figure 6. - Continued.

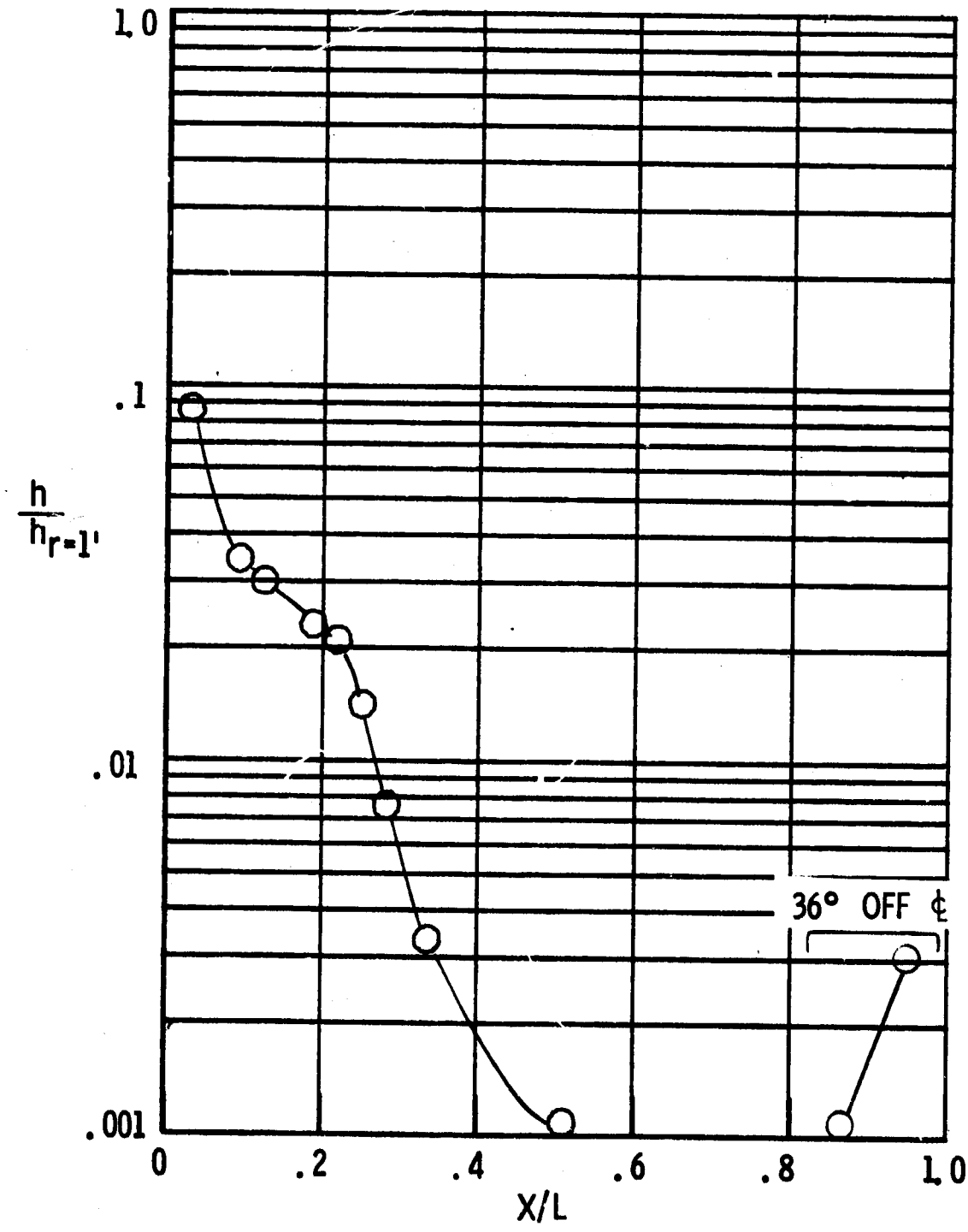

(g) $T_w/T_t = 0.423$

Figure 6. - Concluded.

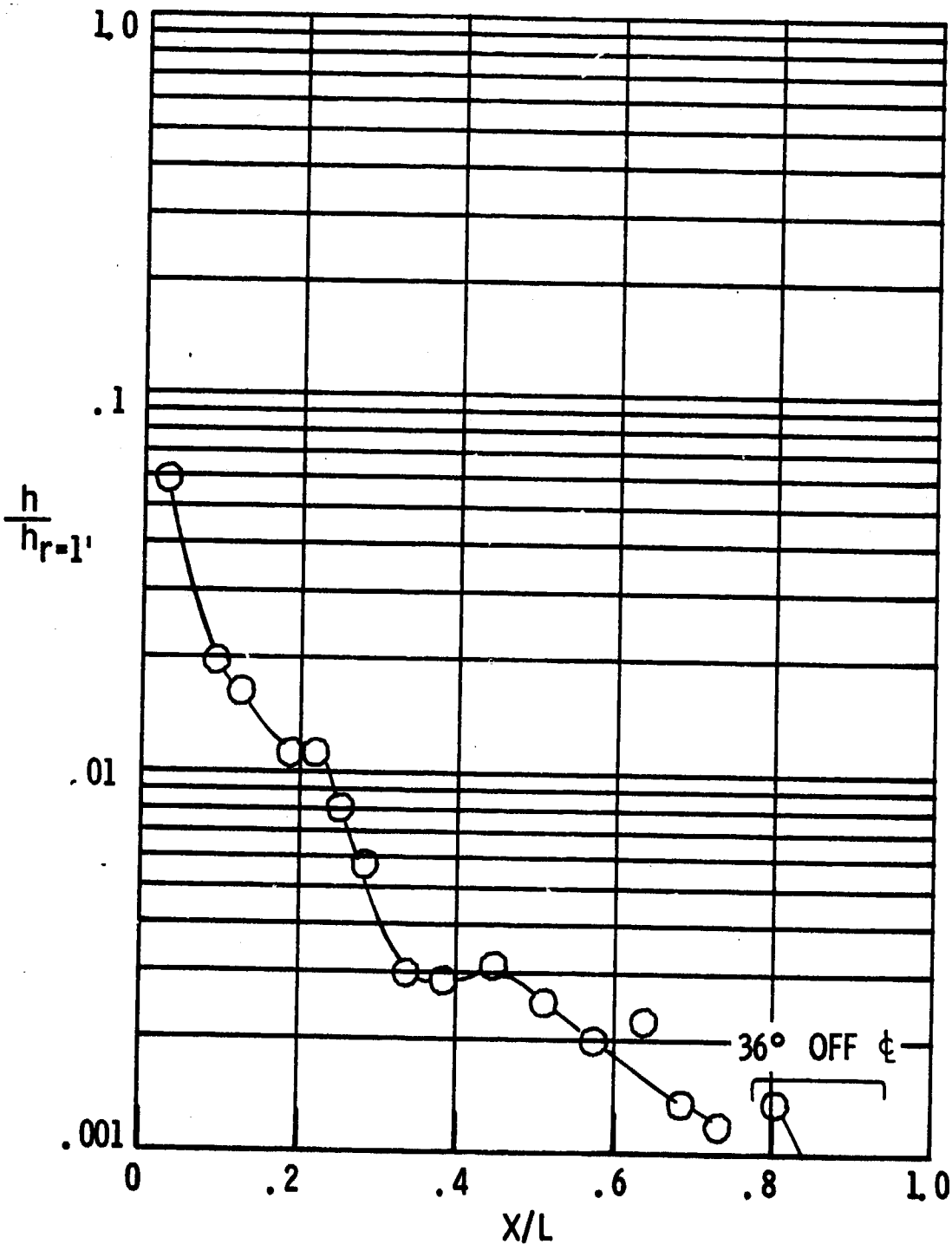

(a) $T_w/T_t = 0.173$

Figure 7. - Leeside centerline heat transfer distribution, $\alpha = 20°$.

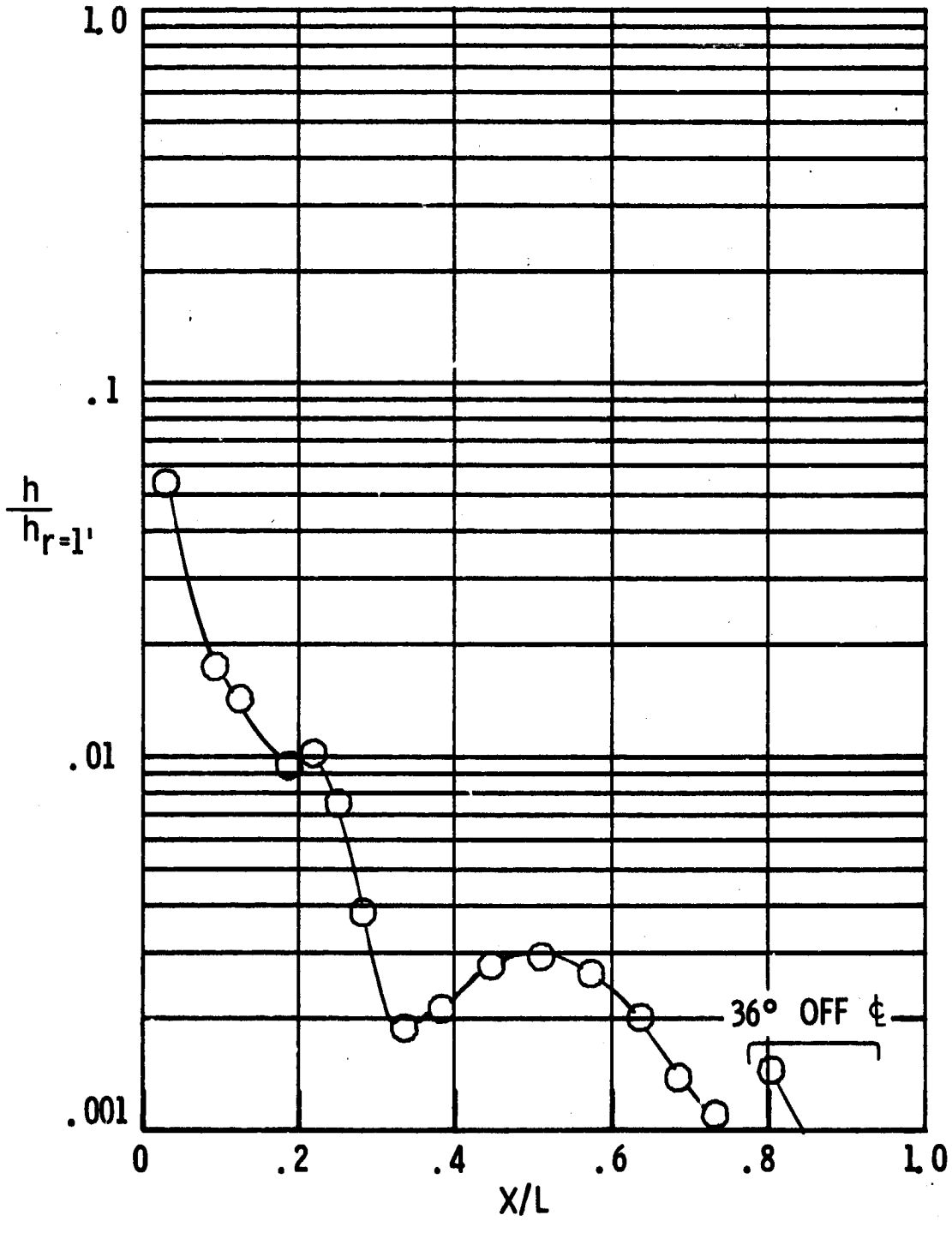

(b) $T_w/T_t = 0.200$

Figure 7. - Continued.

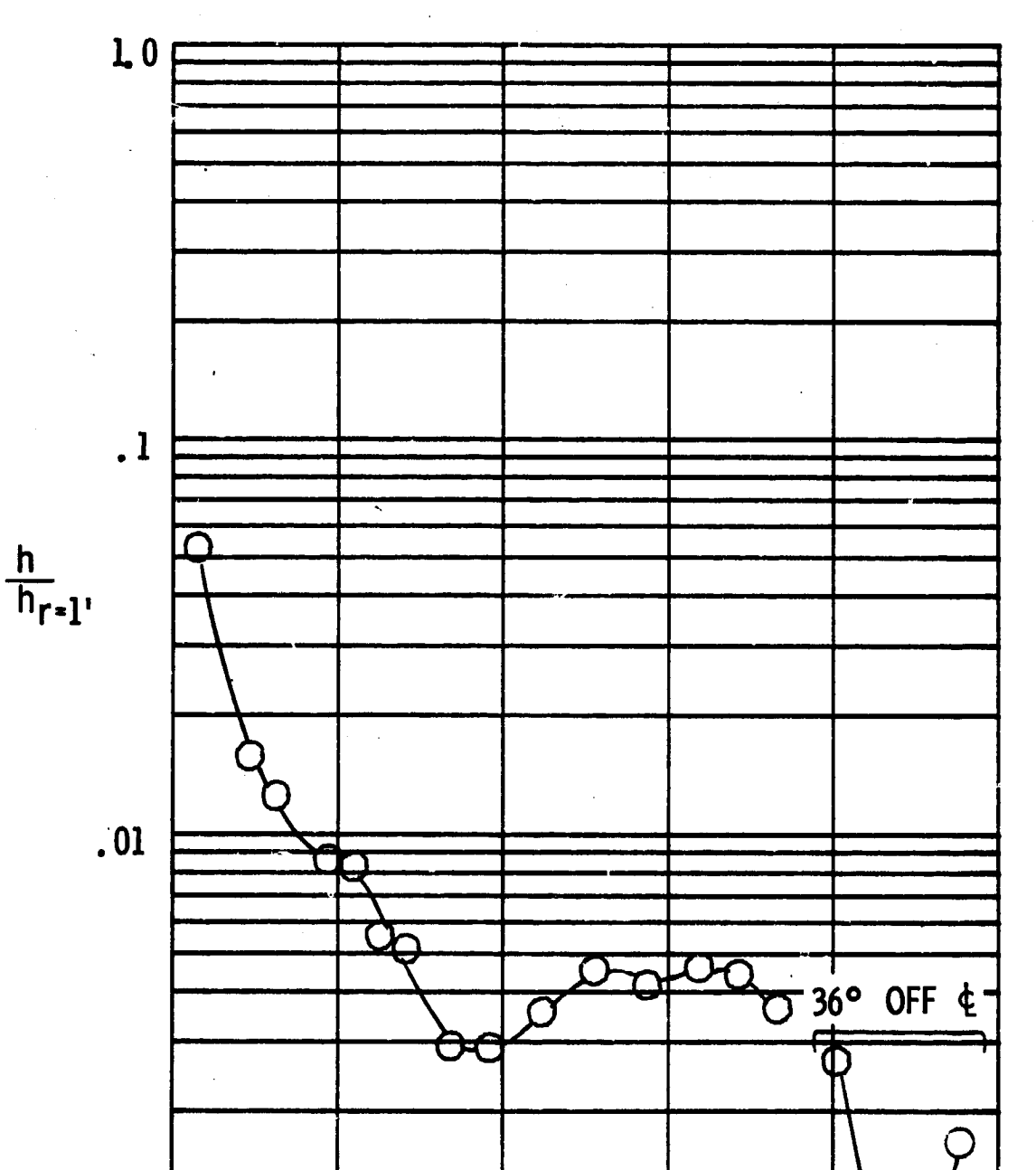

(c) $T_w/T_t = 0.244$

Figure 7. - Continued.

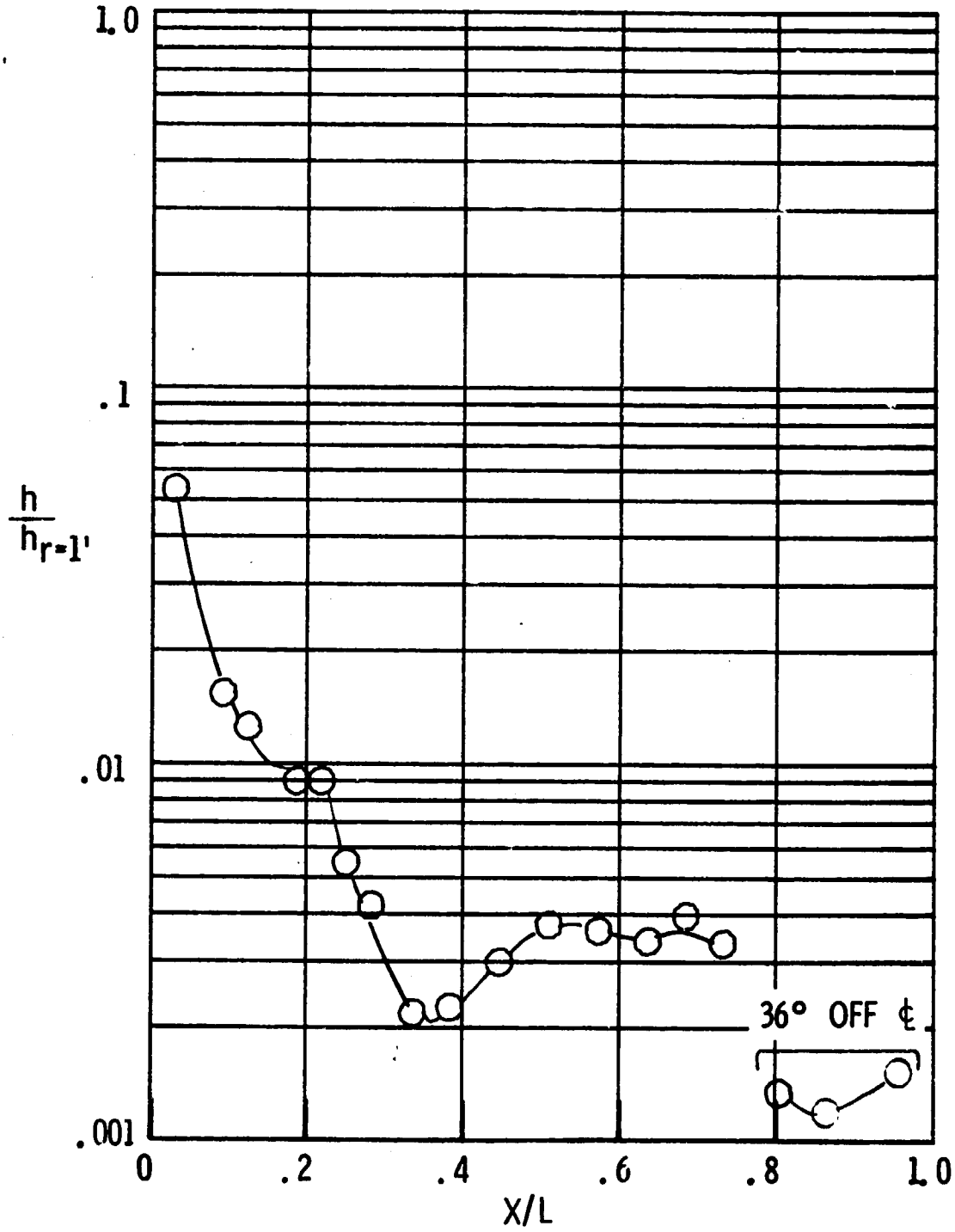

(d) $T_w/T_t = 0.267$

Figure 7. - Continued.

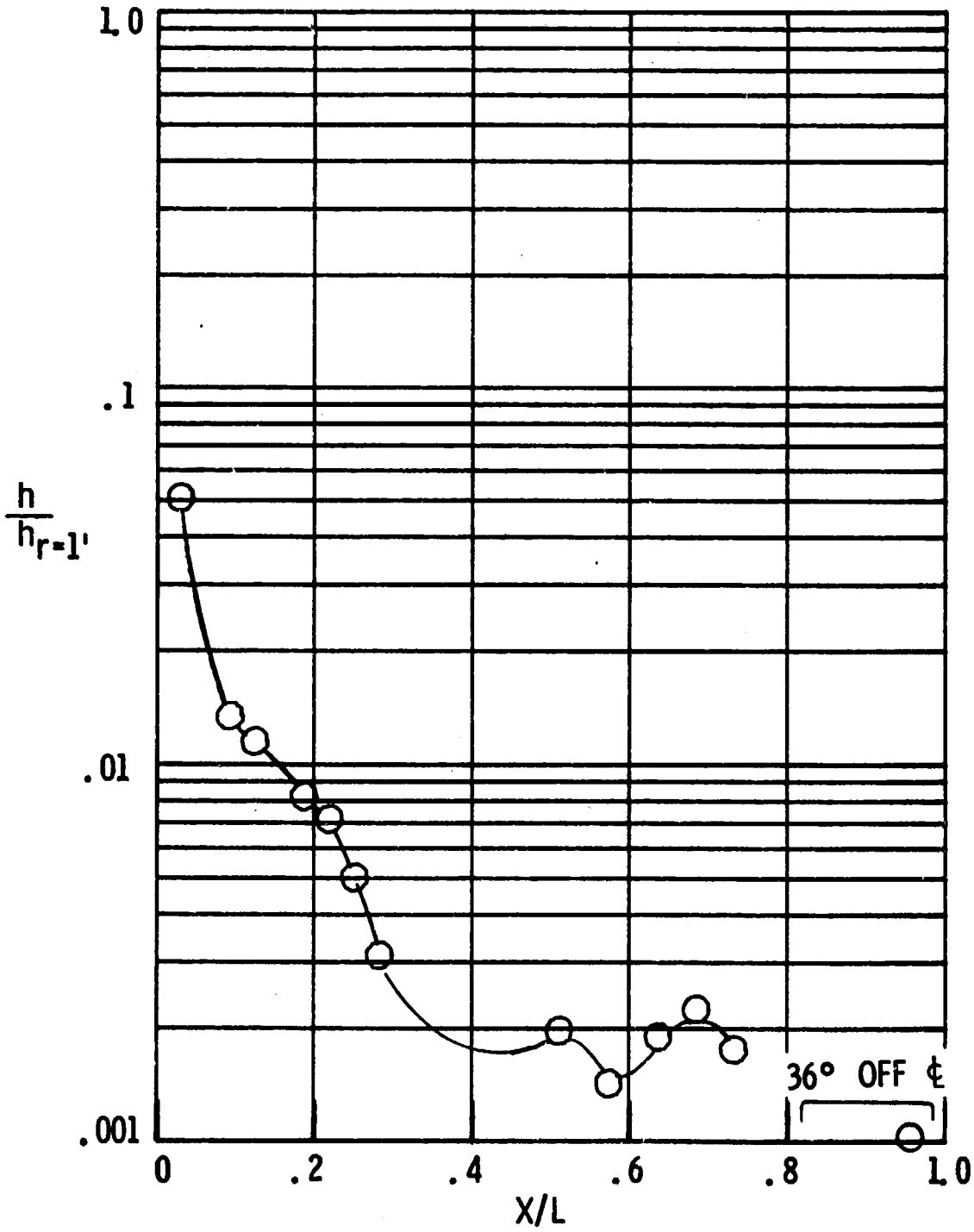

(e) $T_w/T_t = 0.308$

Figure 7. - Continued.

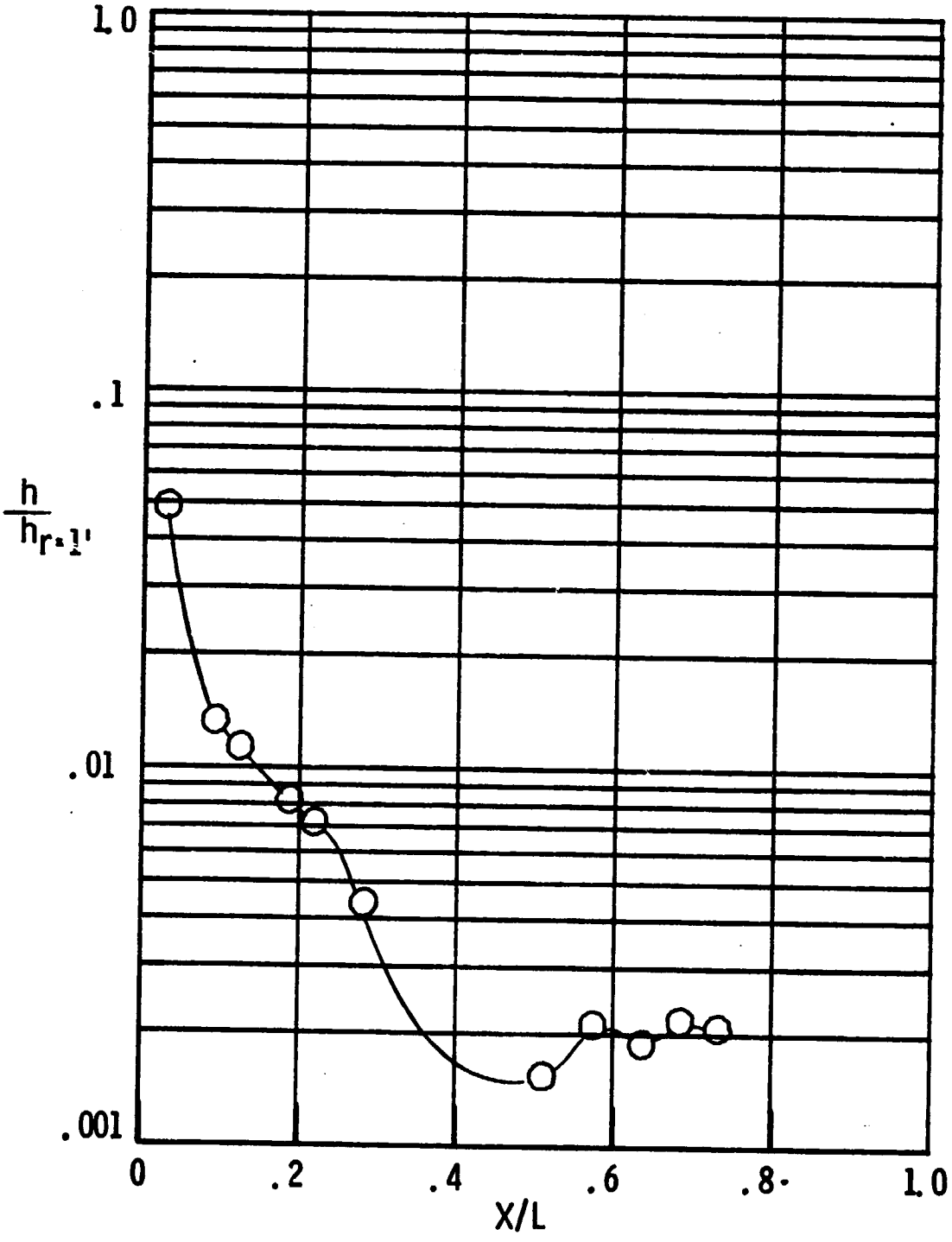

(f) $T_w/T_t = 0.377$

Figure 7. - Continued.

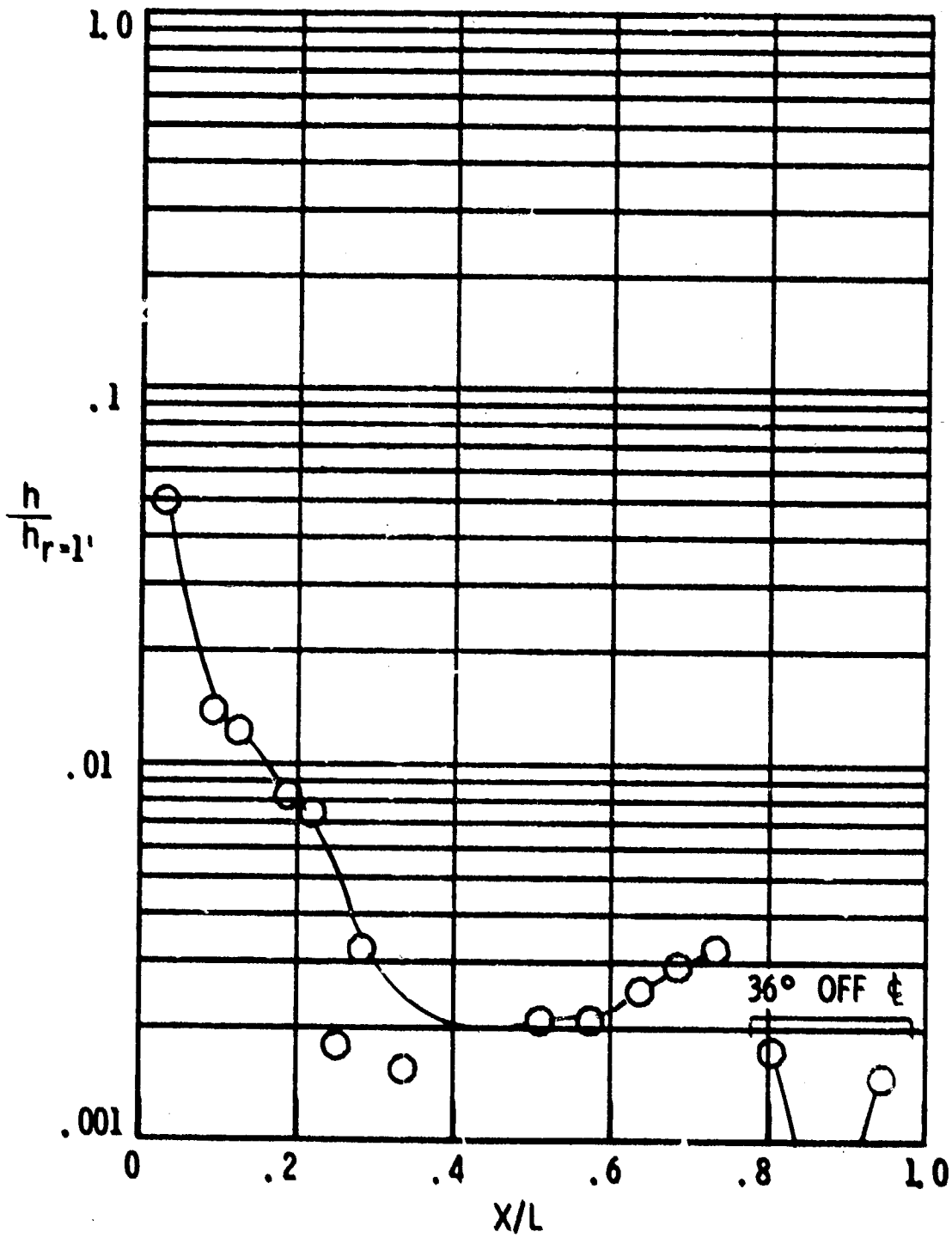

(g) $T_w/T_t = 0.429$

Figure 7. - Concluded.

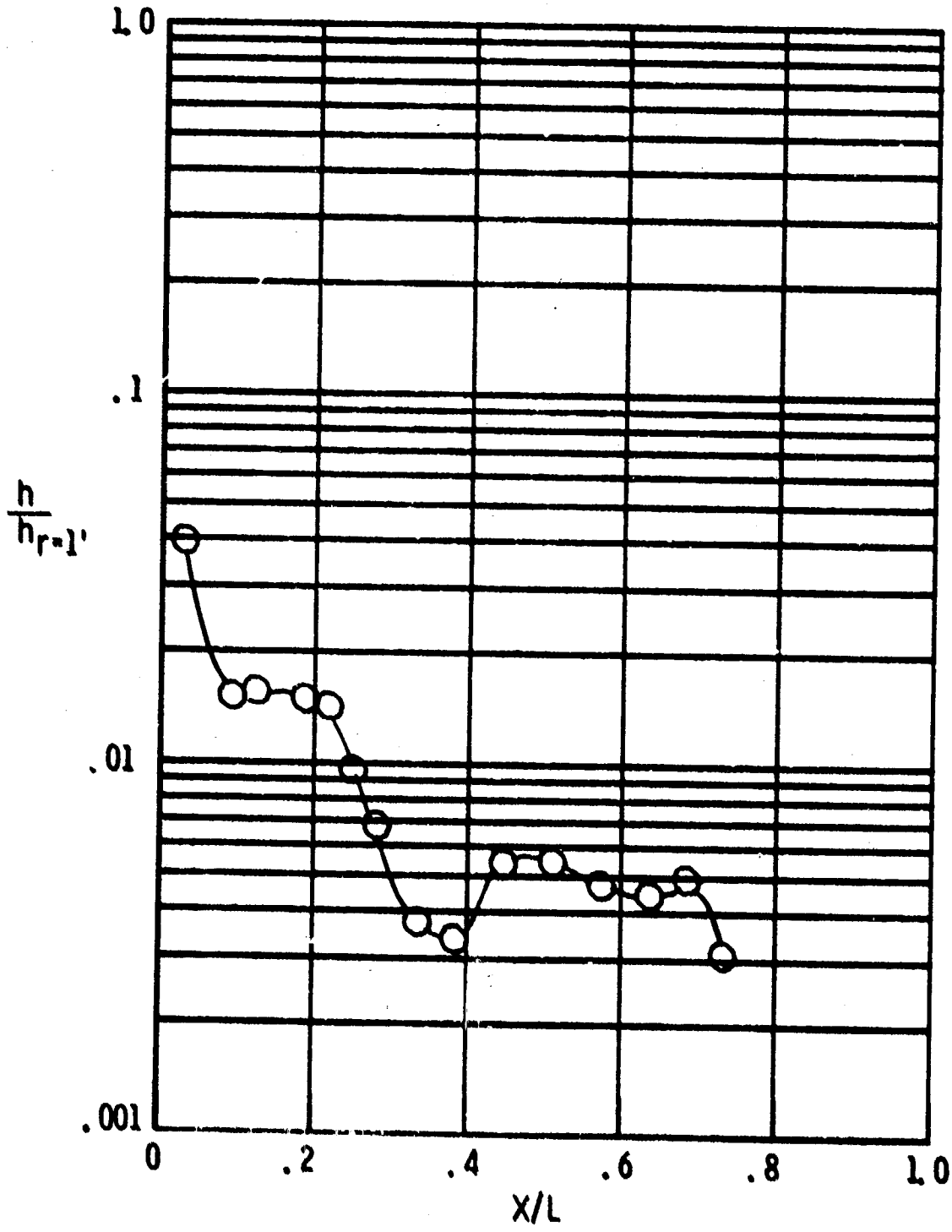

(a) $T_w/T_t = 0.171$

Figure 8. - Leeside centerline heat transfer distribution, $\alpha = 30°$.

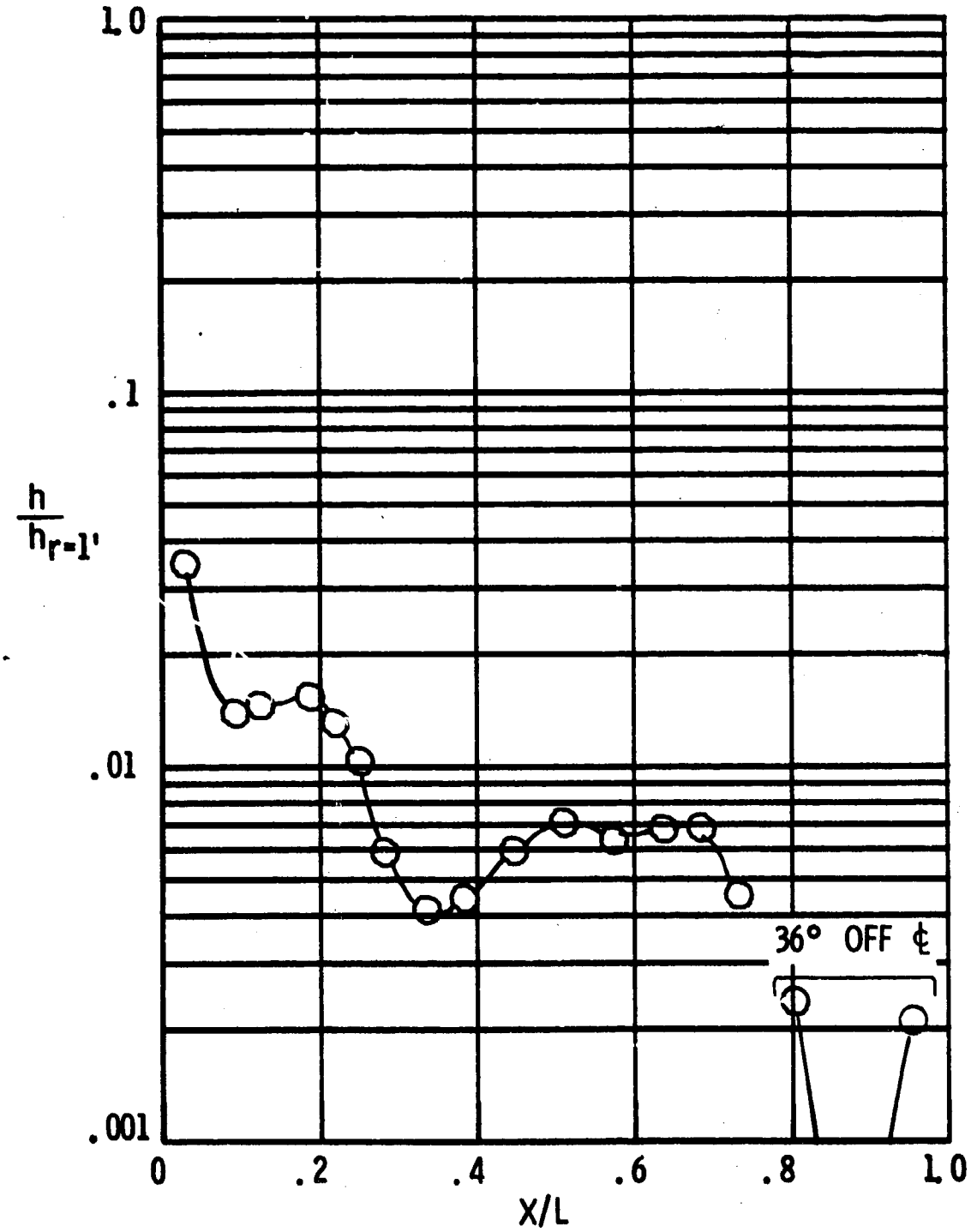

(b) $T_w/T_t = 0.206$

Figure 8. - Continued.

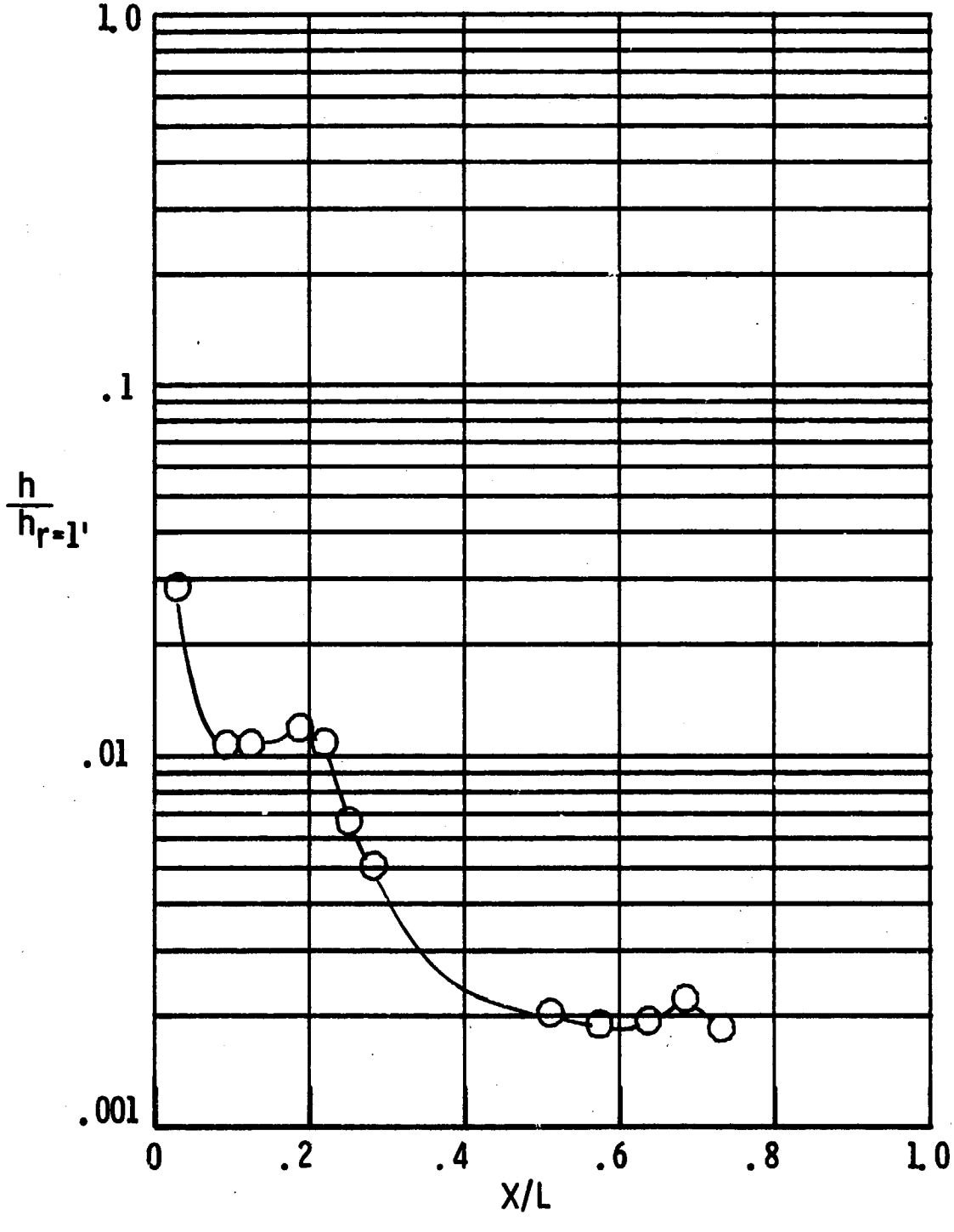

(c) $T_w/T_t = 0.256$

Figure 8. - Continued.

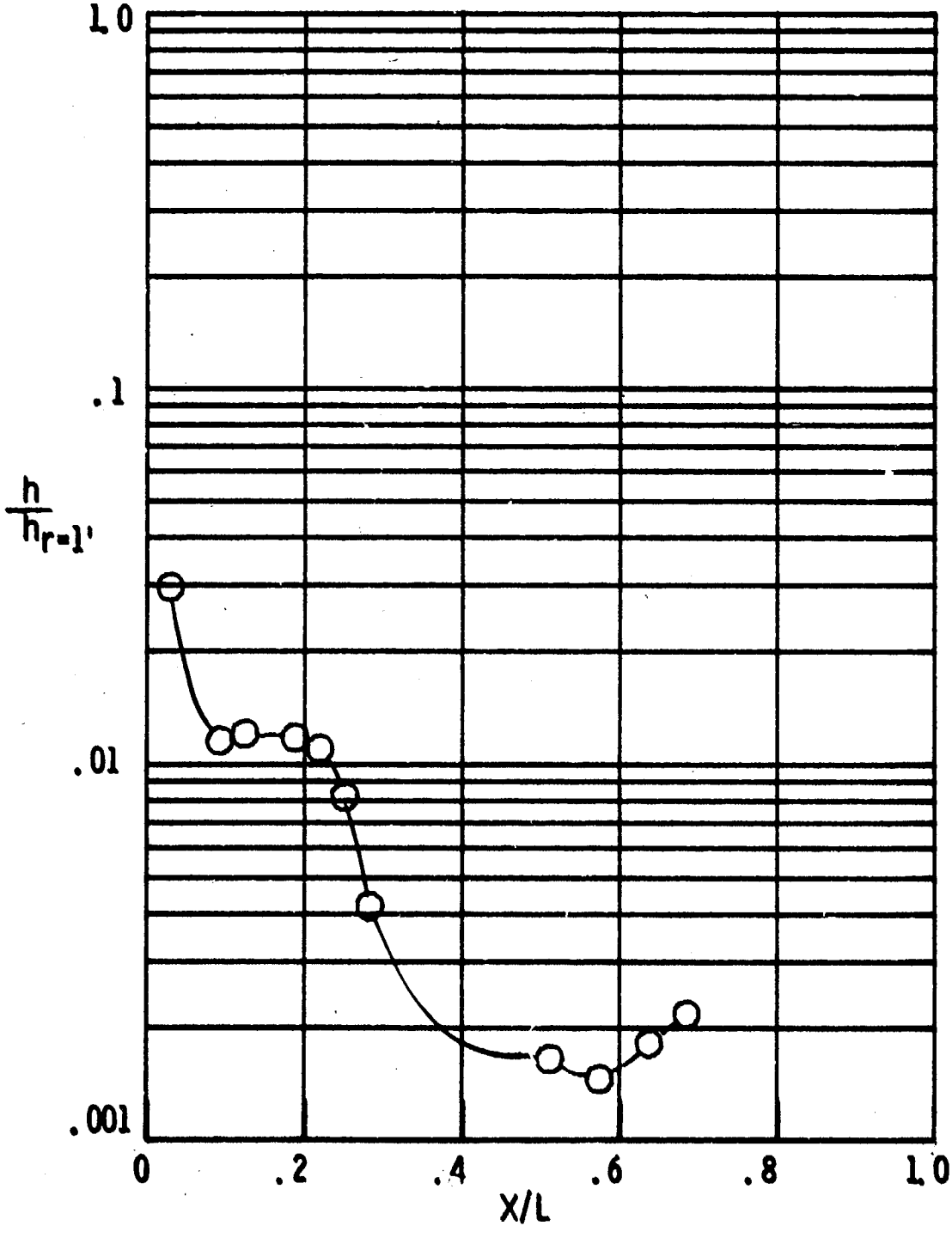

(d) $T_w/T_t = 0.259$

Figure 8. - Continued.

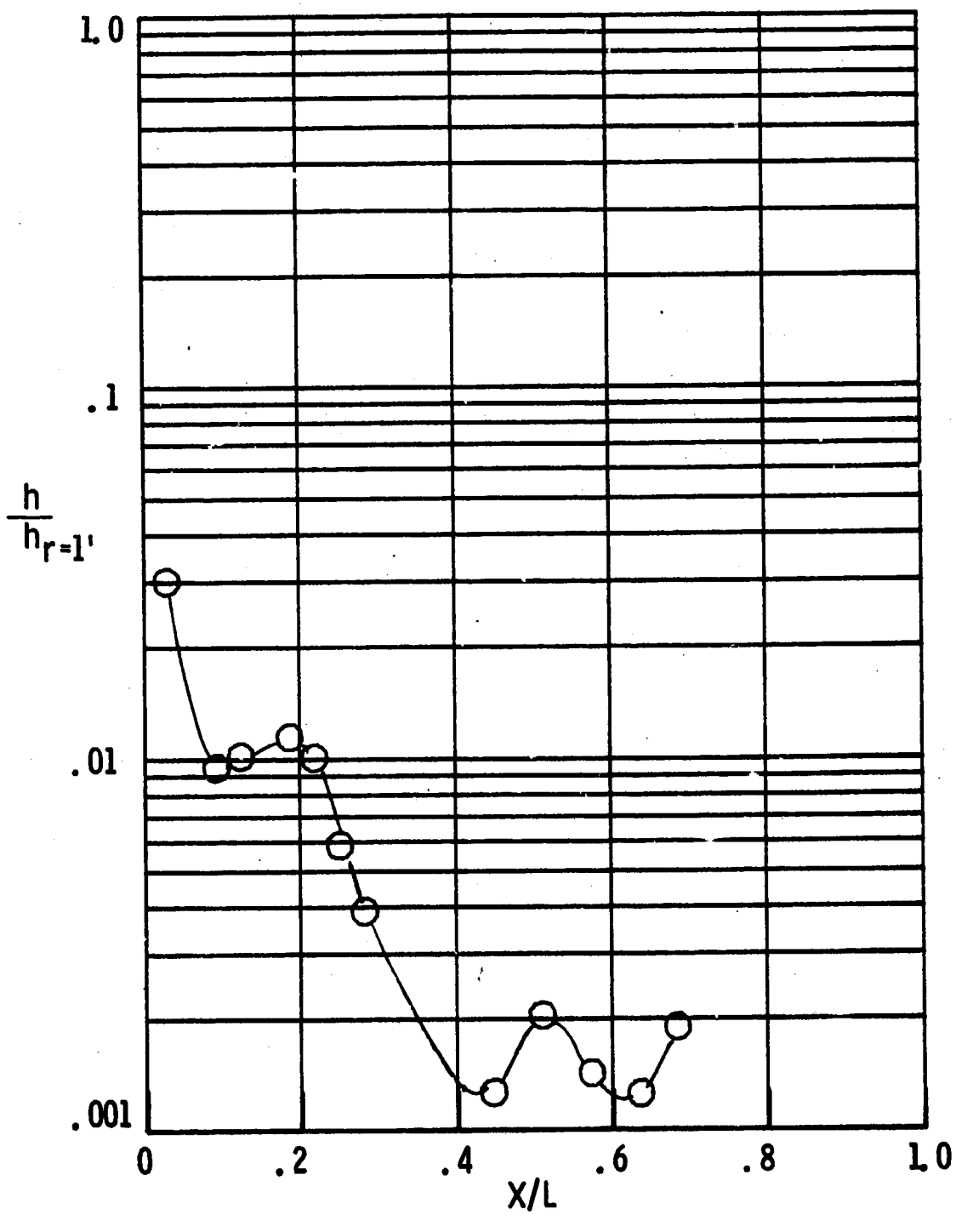

(e) $T_w/T_t = 0.330$

Figure 8. - Continued.

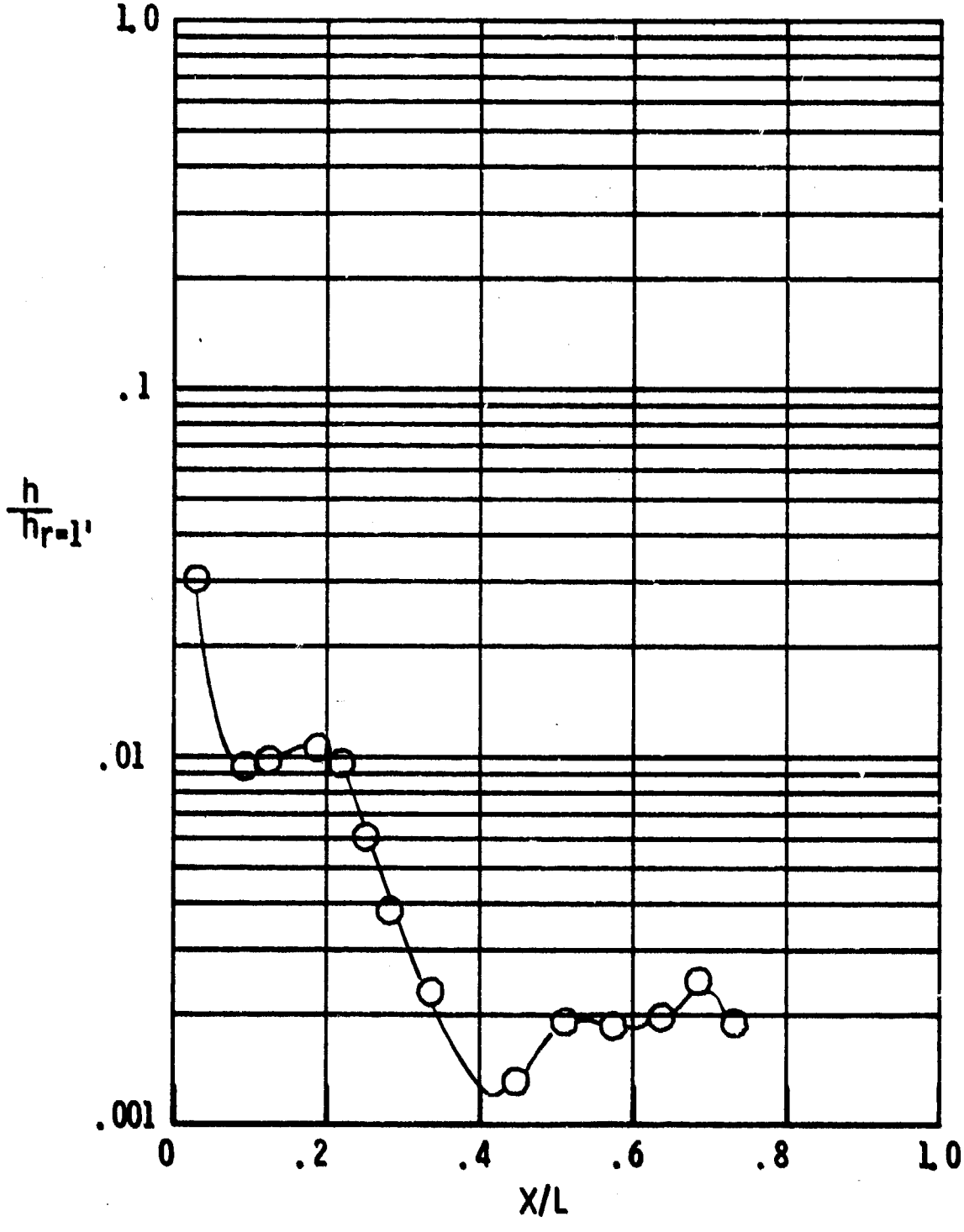

(f) T_w/T_t = 0.380

Figure 8. - Continued.

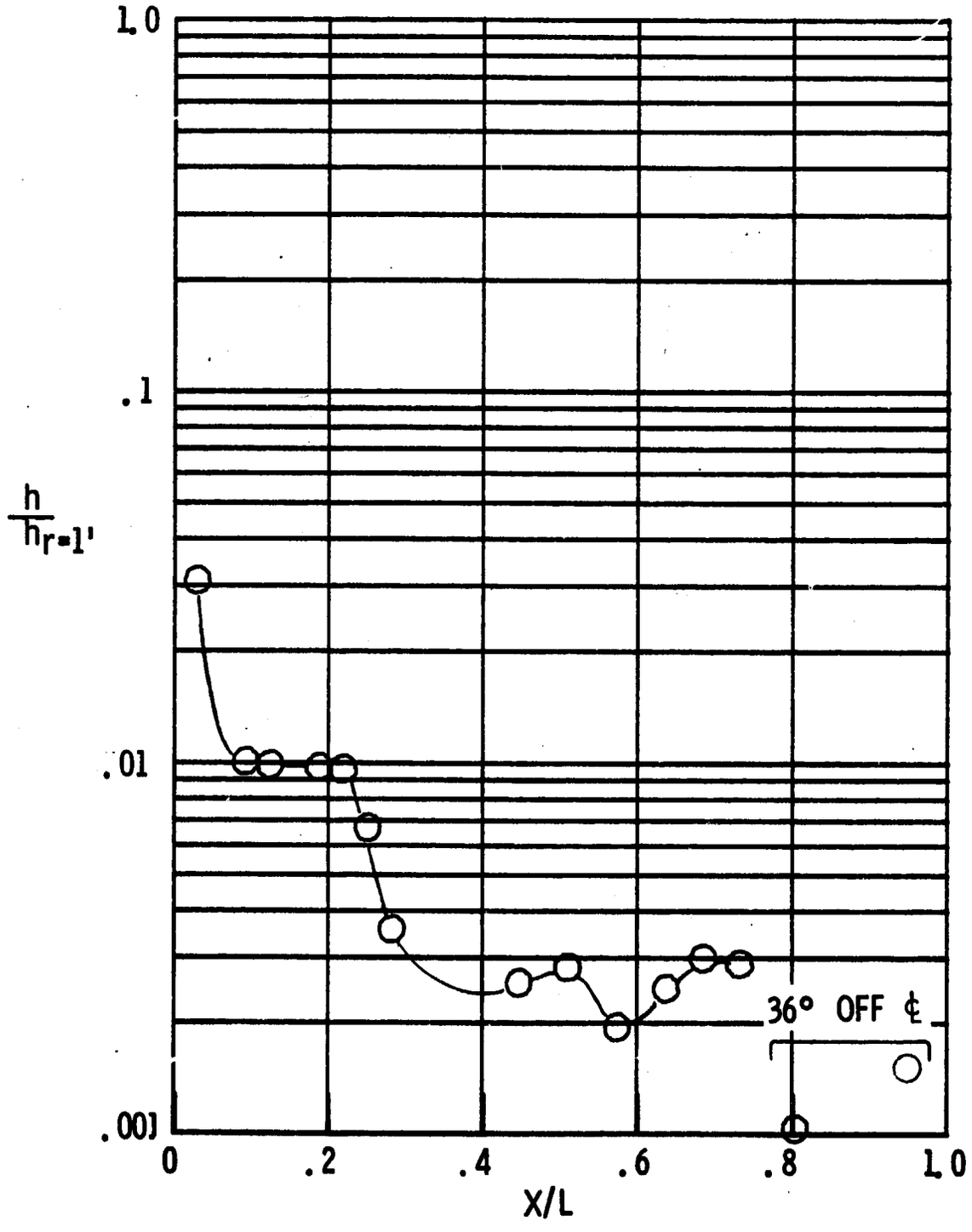

(g) $T_w/T_t = 0.428$

Figure 8. - Concluded.

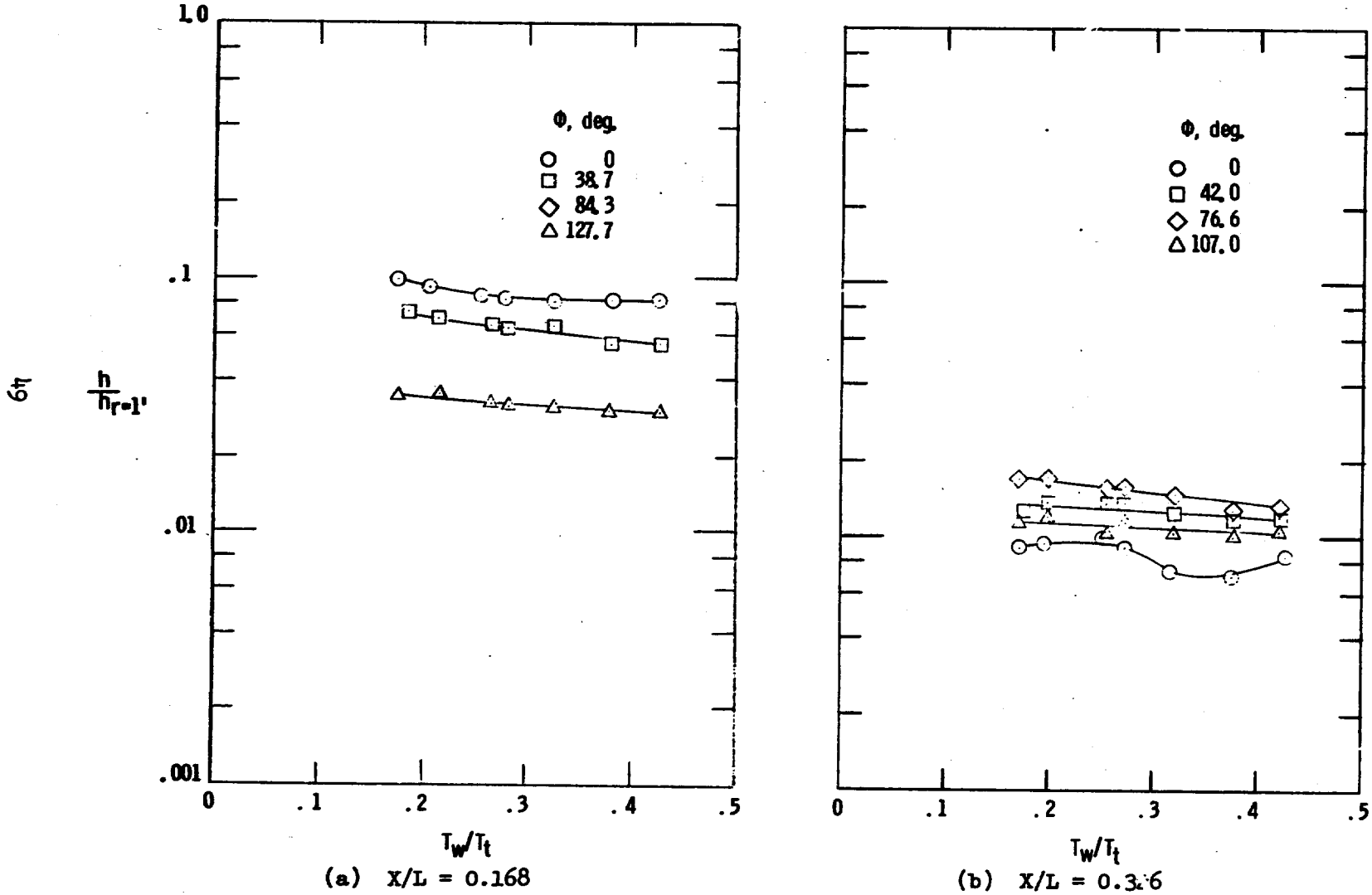

(a) X/L = 0.168

(b) X/L = 0.336

Figure 9. - Variation of heat transfer with wall temperature ratio, α = 0°.

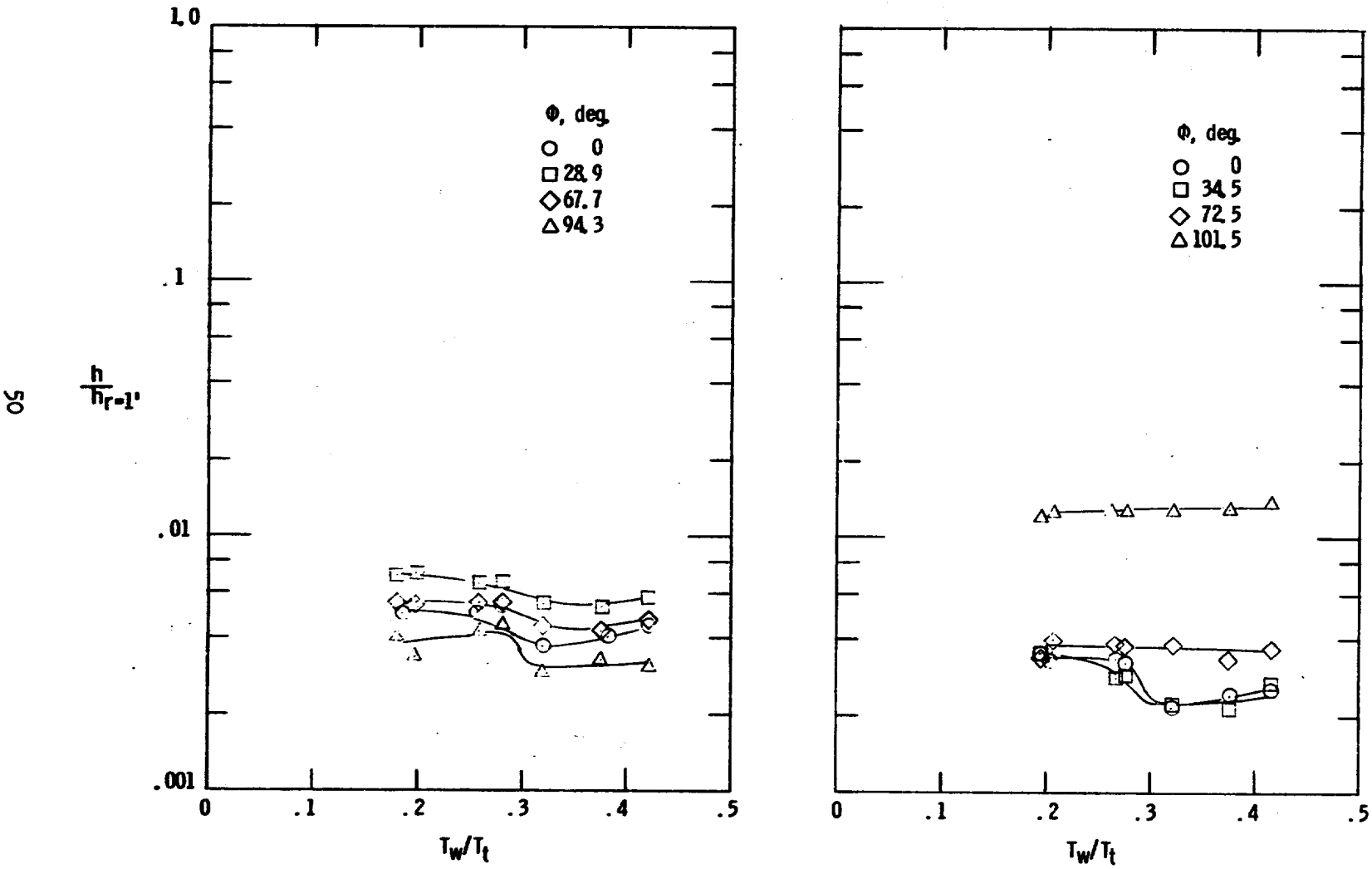

(c) X/L = 0.489

(d) X/L = 0.684

Figure 9. - Concluded.

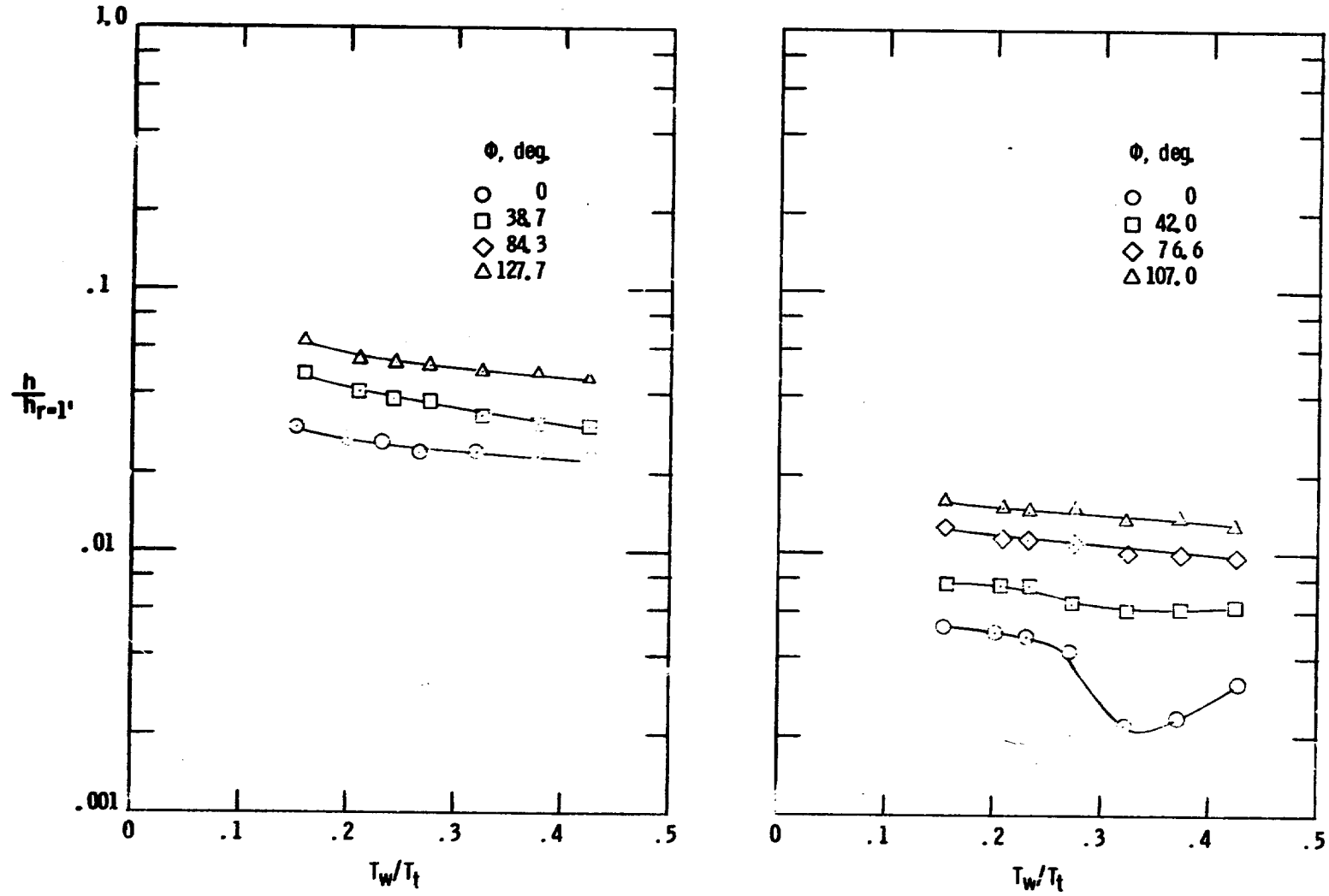

(a) X/L = 0.168

(b) X/L = 0.326

Figure 10. - Variation of heat transfer with wall temperature ratio, α = 10°.

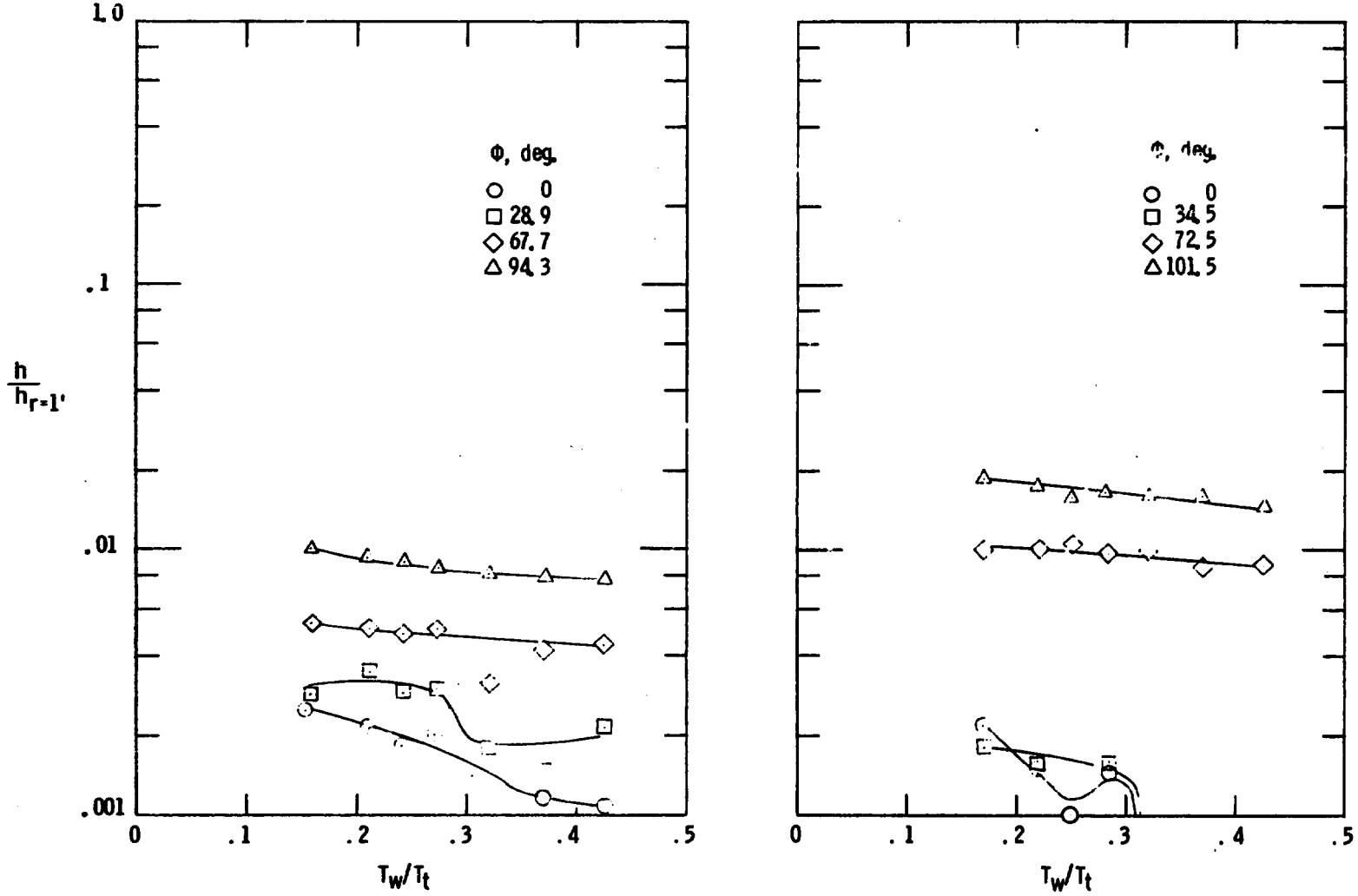

(c) X/L = 0.489

(d) X/L = 0.684

Figure 10. - Concluded.

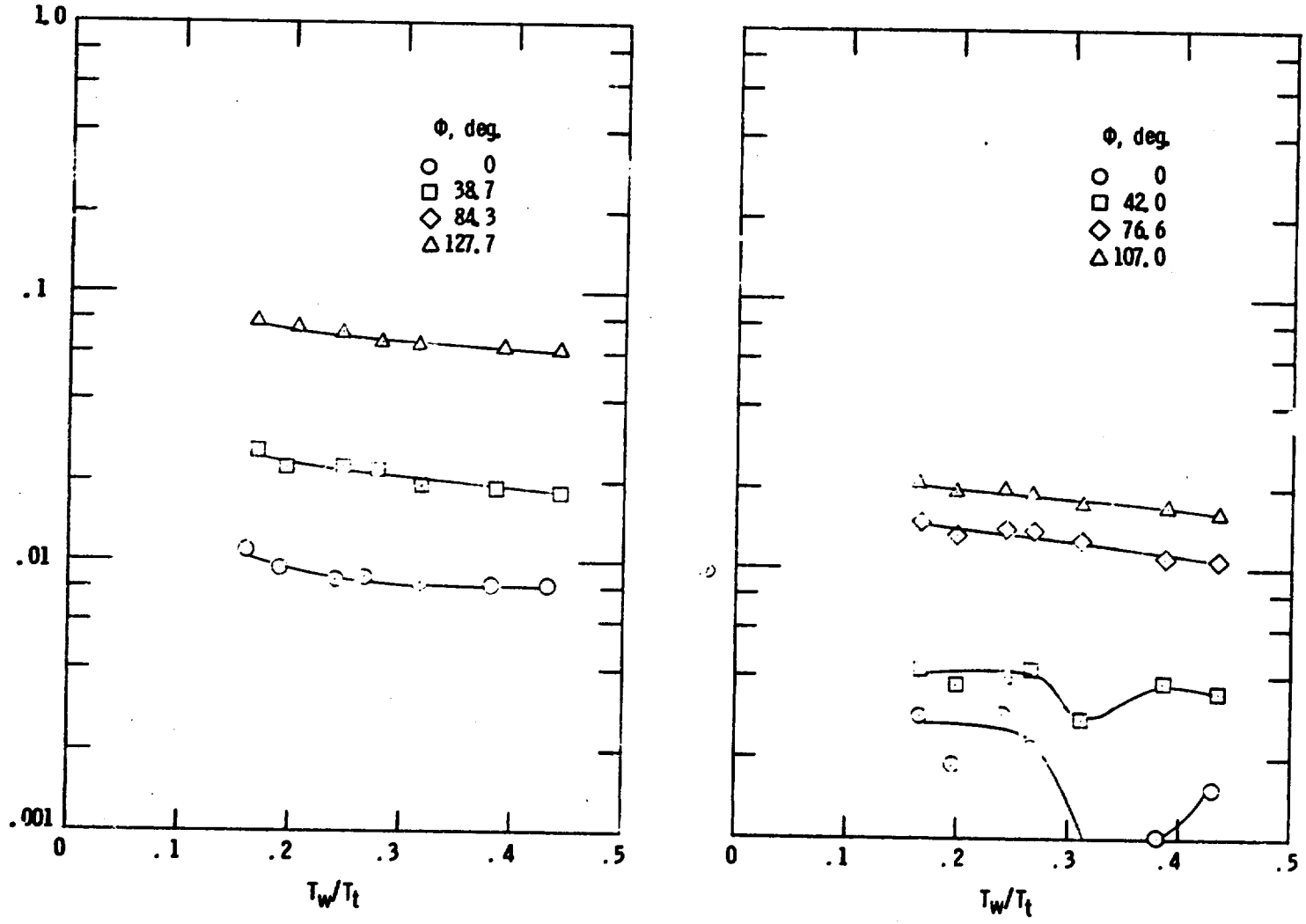

(a) X/L = 0.168

(b) X/L = 0.325

Figure 11. - Variation of heat transfer with wall temperature ratio, α = 20°.

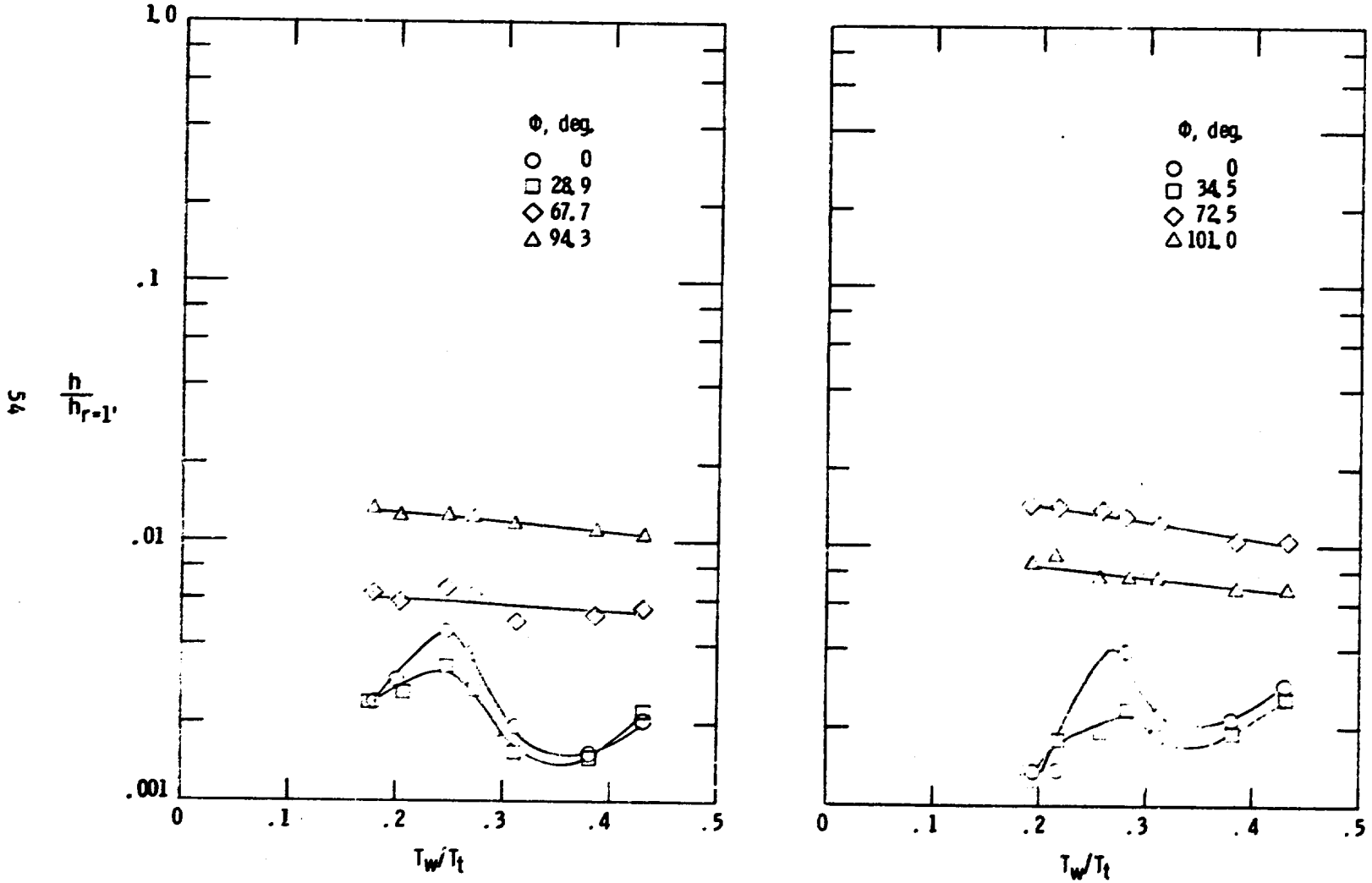

(c) X/L = 0.489

(d) X/L = 0.684

Figure 11. - Concluded.

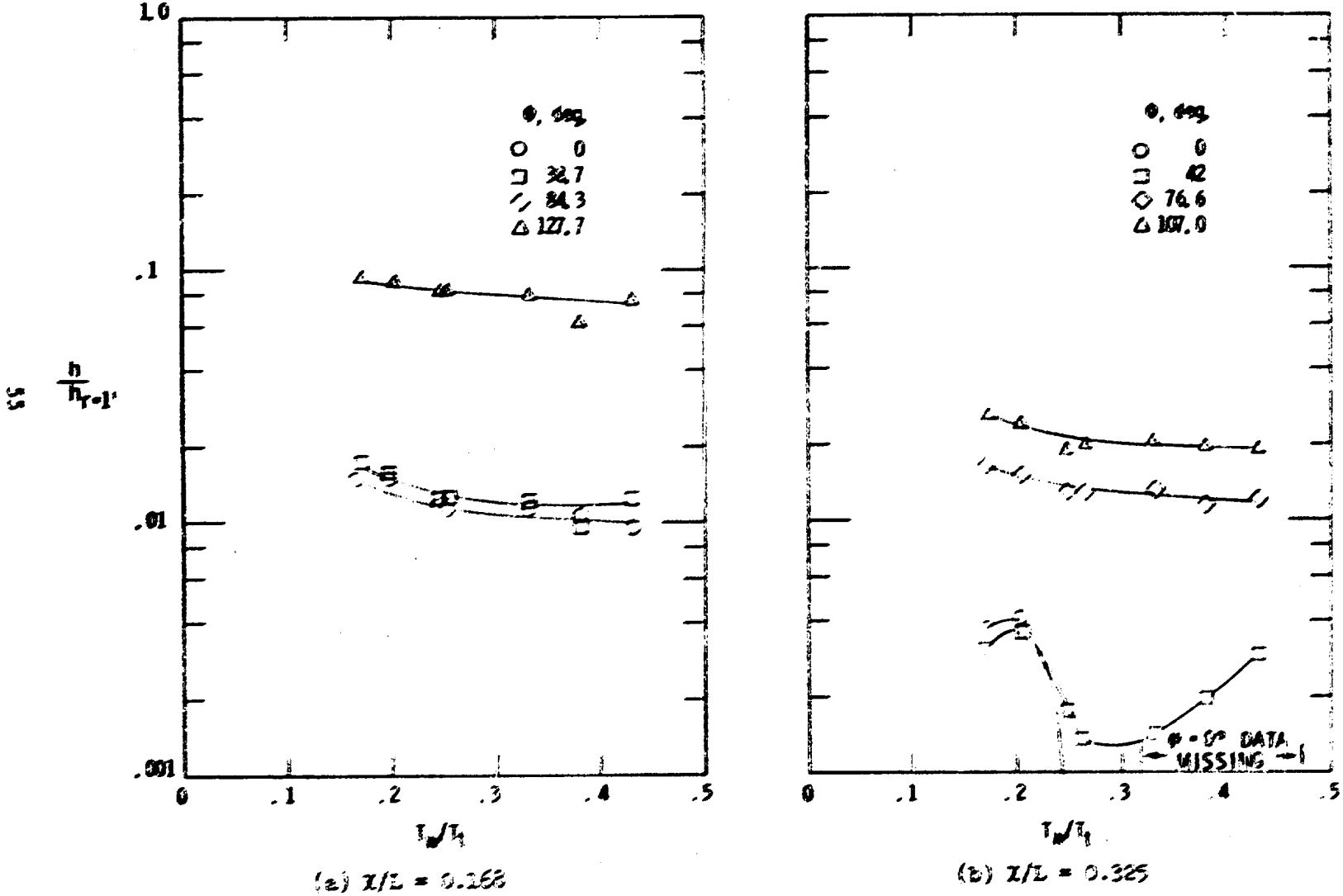

(a) X/L = 0.168

(b) X/L = 0.325

Figure 12. - Variation of heat transfer with wall temperature ratio, $\alpha = 30°$.

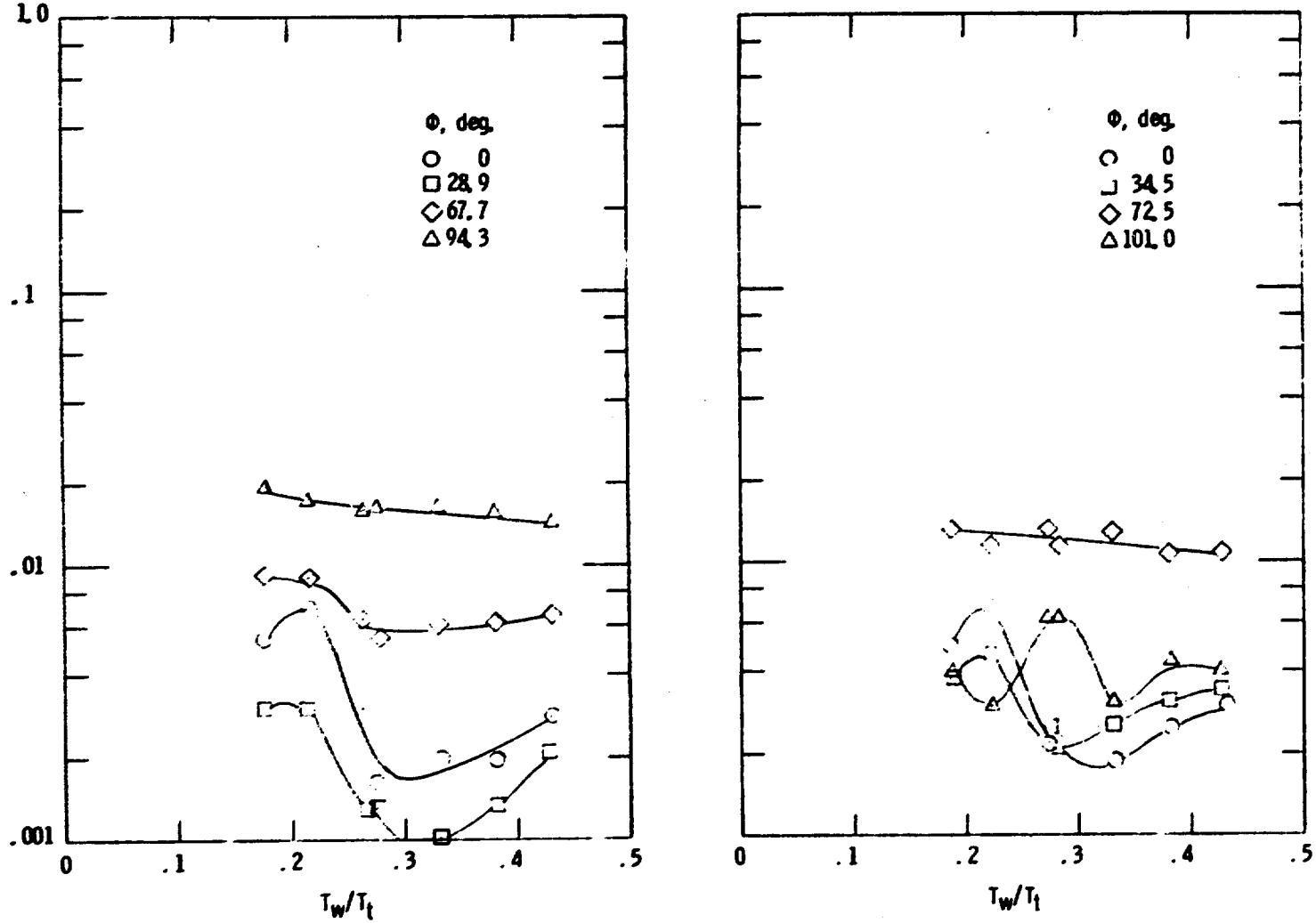

(c) X/L = 0.489

(d) X/L = 0.684

Figure 12. - Concluded.